Identifying Sialylation Linkages at the Glycopeptide Level by Glycosyltransferase Labeling Assisted Mass Spectrometry (GLAMS)

He Zhu[†], Shuaishuai Wang[†], Ding Liu[†], Lang Ding[†], Congcong Chen[†], Yunpeng Liu[†], Zhigang Wu[†], Roni Bollag[‡], Kebin Liu[§], Jun Yin[†], Cheng Ma[†], Lei Li[*†] , Peng George Wang[*†,¶]

[†] Department of Chemistry, Georgia State University, Atlanta, GA 30303, United States

[‡] Georgia Cancer Center, Augusta University, Augusta, GA 30912, United States

[§] Department of Biochemistry and Molecular Biology, Augusta University, Augusta, GA 30912, United States

[¶] Current address: Department of Chemistry, Southern University of Science and Technology, Shenzhen 518055, China.

ABSTRACT

Precise assignment of sialylation linkages at the glycopeptide level is of importance in bottom-up glycoproteomics, and is also an indispensable step to understand the function of glycoproteins in pathogen-host interactions and cancer progression. Even though some efforts have been dedicated to the discrimination of α2,3/α2,6-sialylated isomers, unambiguous identification of sialoglycopeptide isomers is still needed. Herein, an innovative strategy of glycosyltransferase labeling assisted mass spectrometry (GLAMS) were developed. After specific enzymatic labeling, oxonium ions from higher-energy C-trap dissociation (HCD) fragmentation of α2,3-sailoglycopeptides generate unique reporters to distinctly differentiate those of α2,6-sailoglycopeptide isomers. Using this strategy, a total of 1,138 linkage-specific sialoglycopeptides were successfully identified from 126 glycoproteins in human serum.

INTRODUCTION

Glycosylation is one of the most important post-translational modifications (PTMs) of proteins[1]. It plays an indispensable role in a wide variety of biological and physiological processes including protein folding[2], cellular communication and signaling[3], immune response[4], and pathogen-host interactions[5]. It was estimated that more than half of proteins in the human proteome are glycosylated[6]. Glycosylation is generally classified into N-glycosylation and mucin-type O-glycosylation. In N-glycosylation, the glycans are attached to asparagine residues of proteins in the consensus motif Asn-X-Ser/Thr/Cys (X can be any amino acid except for proline)[7], whereas the glycan moieties are linked to serine or threonine residues of proteins in O-glycosylation[1]. N-acetylneuraminic acid (Neu5Ac) is most common form of diverse sialic acids found on glycan chains in humans[8]. Neu5Ac is the frequently the terminal monosaccharide residue that linked to galactose (Gal) via an α2,3 or an α2,6 linkage[9]. The two Neu5Ac linkage isomers have important roles in pathogen binding. For example, avian influenza A viruses preferentially bind to respiratory epithelial cells that contain α2,3-linked Neu5Ac moieties, while human influenza viruses selectively bind to α2,6-linked Neu5Ac moieties[10]. In addition, altered sialylation linkages is closely correlated with health status. In patients diagnosed with prostate cancer, the structure of sialylated glycans released from the prostate-specific antigen (PSA) is rich in α2,3 linkages, whereas the structure of sialylated glycans from healthy people's PSA is predominantly via α2,6 linkages[11]. Without detailed information on sialylation linkages, it is challenging to decipher the biological functions of sialoglycoproteins.

A variety of methods, including sialidase treatment[12], chemical derivatization[13-21], and mass spectrometry (MS)[22-24], have been used to distinguish α2,3 and α2,6-sialylated glycans, but the location of corresponding glycosylation sites is not evident. The emerging technology of MS-

47 based glycoproteomics[25-29] provides a high-throughput approach to analyze site-specific protein
48 glycosylation. Consequently, strategies for identifying sialylation linkages at the glycopeptide
49 level are required. Established chemical approaches[30, 31] modify not only sialic acids of the
50 glycan moiety but also acidic amino acid residues and the C-terminus of the peptide backbone,
51 which increases the complexity of spectra analysis, especially in relation to large scale
52 glycoproteomics data[32]. Pseudo MS^3 fragmentation[22] and ion mobility-mass spectrometry (IM-
53 MS)[33] have also been applied to distinguish sialoglycopeptide isomers but this technology has
54 not been **demonstrated (**?effective) for large-scale glycopeptides analysis. Even though the
55 fragmentation of high energy C-trap dissociation (HCD) can achieve the high-throughput
56 assignment of α2,3/α2,6-sialoglycopeptide isomers, there are still many ambiguous
57 glycopeptides without sialylation linkage information[34].

58 Enzymatic labeling has become a promising tool for probing proteins with specific
59 glycosylation because of its high specificity and mild reaction condition[35-41]. In our previous
60 research, a β1,4-N-acetylgalactosaminyltransferase from *Campylobacter jejuni* (CgtA) was
61 demonstrated to specifically recognize the Neu5Ac(α2,3)Gal epitope and transfer N-
62 acetylgalactosamine (GalNAc) or N-azidoacetylgalactosamine (GalNAz) to Gal residue via β1,4
63 linkage[42]. Taking advantage of the specificity of CgtA, we herein report a new strategy for
64 identification of α2,3 and α2,6 sialoglycopeptide isomers by glycosyltransferase labeling assisted
65 mass spectrometry (GLAMS). As shown in **Scheme 1**, sialoglycopeptides (monosialylation for
66 example) without linkages information were treated with GalNAz labeling by CgtA. After HCD
67 fragmentation, if only the oxonium ions of HexNAc (N-acetylhexosamine, m/z 204) and Neu5Ac
68 (m/z 292) are observed in the spectrum, this identifies an α2,6 linkage; if one more oxonium ion
69 m/z 245 from GalNAz is included, then it represents an α2,3 linkage. We demonstrated the

70 capacity of GLAMS to effectively differentiate α2,3/α2,6 isomers using synthetic
71 sialoglycopeptides, and applied it to profile sialylated N-glycopeptides digested from serum
72 samples, in which we identified 1,138 linkage specific sialoglycopeptides with the modified
73 pGlyco 2.0 software[27].
74
75 **EXPERIMENTAL SECTION**
76 **Chemicals and materials**
77 Amicon Ultra-0.5 Centrifugal Filter Unit with NMWL of 30 kD was obtained from
78 Millipore Sigma (St. Louis, MO). iSPE® HILIC SPE Cartridge was purchased from The Nest
79 Group (Southborough, MA). XAmide medium was provided by Dr. Xinmiao Liang's lab (Dalian
80 Institute of Chemical Physics, Chinese Academy of Sciences). Sequencing grade porcine trypsin
81 was purchased from Promega (Madison, WI); Deionized water was produced by a Milli-Q A10
82 system from Millipore (Bedford, MA). Optimal LC-MS grade quality acetonitrile (ACN), formic
83 acid (FA) and water were purchased from Thermo Fisher Scientific, Inc. (Waltham, MA).
84 Dithiothreitol (DTT), 2-Iodoacetamide (IAA) and trifluoroacetic acid (TFA) were bought from
85 Alfa Aesar (Ward Hill, MA). Ammonium bicarbonate (NH_4HCO_3) was purchased from
86 Millipore Sigma (St. Louis, MO). All other chemicals of analytical grade were commercially
87 available.
88 Sialylated oligosaccharide standards including 3'-sialyllactose (3SL) and 6'-sialyllactose
89 (6SL) were enzymatically synthesized using *Pasteurella multocida* α2,3-sialyltransferase 1 and
90 *Photobacterium damselae* α2,6-sialyltransferase as described before[43].
91 Serum samples from four healthy people, ten patients with colon cancer and four patients
92 with liver cancer were provided by Georgia Cancer Center at Augusta University and stored at -

93 80 °C until use. The protocol for serum sample preparation was approved by the Institutional
94 Review Board of Augusta University and was performed in accordance with the Helsinki
95 Declaration. All participants gave written informed consents.

96 **Protein digestion**

97 The protein digestion was performed using a filter aided sample preparation (FASP)[44]
98 method with minor modification. Approximately 1 mg of total proteins from human serum was
99 subjected to FASP procedures. Samples were denatured in 20 μL of lysis buffer (4% SDS, 100
100 mM DTT, 20 mM Tris-HCl, pH 7.6) at 95 °C for 10 min. When the solution was cooled down to
101 room temperature, 1 mL of UA solution (8 M urea, 20 mM Tris-HCl, pH 8.5) was added. The
102 solution was gradually transferred into a 30 kD filter and centrifugated at 15,000 rpm at 20 °C
103 for 15 min. Then 100 μL of IAA solution (50 mM IAA in UA solution) was added to the filter
104 and incubated for 30 min in the darkness followed by centrifugation at 15,000 rpm for 10 min.
105 After that, 100 μL of UA solution and 200 μL of digestion buffer (100 μL of 50 mM NH_4HCO_3
106 each time) were added and centrifuged at 15,000 rpm for 10 min, respectively. Finally, 20 μg of
107 trypsin was added into the filter and incubated at 37 °C for 12 h. The tryptic peptides were eluted
108 using 100 μL of 50 mM NH_4HCO_3 for six times. The concentration of the collected peptides was
109 measured based on absorbance at 280 nm with Nanodrop. Five hundred μg of the peptides were
110 taken and subsequently dried in Vacufuge at room temperature, then were lyophilized twice to
111 remove NH_4HCO_3. The dried samples were stored at −20 °C for further use.

112 **Enrichment of glycopeptides**

113 The enrichment of glycopeptides was performed using an iSPE HILIC cartridge by the
114 procedure of ZIC-HILIC[45]. Briefly, the HILIC cartridge was pre-washed with 300 μL of 0.1%
115 TFA and conditioning with 600 μL of 80% ACN containing 0.1% TFA. Peptide samples

116 dissolved in 400 μL of 80% ACN containing 0.1% TFA were loaded onto the cartridge. The
117 flow-through was reloaded onto the column for another two times. Then the column was washed
118 with 1.2 mL of 80% ACN containing 1% TFA. The glycopeptides were eluted using 750 μL of
119 0.1% TFA, 60 μL of H_2O, 60 μL of 25 mM NH_4HCO_3 and 60 μL of 50% ACN. The fractions
120 were combined followed by lyophilization and stored at -20 °C.

121 **Enzymatic labeling of glycopeptides**

122 The β1,4-N-acetylgalactosaminyltransferase from *C. jejuni* (CgtA) and sugar nucleotide
123 UDP-N-azidoacetylgalactosamine (UDP-GalNAz) were prepared as described previously[42]. For
124 enzymatic labeling, the 40 μL reaction mixture containing the enriched glycopeptides, 50 mM
125 Tris-HCl buffer (pH 7.5), 5 mM $MgCl_2$, 200 μM UDP-GalNAz and 10 μg CgtA was incubated
126 in a 37 °C water bath for 1 h. The reaction was quenched by adding 60 μL of ACN, 6 μL of 10%
127 TFA and 215 μL of ACN containing 1% TFA. Then the glycopeptides were purified with an in-
128 house packed Amide HILIC microcolumn (6 mg of XAmide HILIC medium in a 200 μL tip)
129 which was preconditioned with 100 μL of 0.1% TFA and 200 μL of 85% ACN containing 0.1%
130 TFA. After loading the reaction mixture onto the tip column, the column was washed with 100
131 μL of 85% ACN, 0.1% TFA to remove salts and proteins. The glycopeptides were collected
132 using 200 μL of 0.1% TFA and lyophilized.

133 **Nano LC-MS/MS analysis**

134 Nano RP HPLC-MS experiments were performed on an LTQ-Orbitrap Elite mass
135 spectrometer (Thermo Fisher) equipped with EASY-spray source and nano-LC UltiMate 3000
136 high-performance liquid chromatography system (Thermo Fisher). The separation was
137 performed on an EASY-Spray PepMap C18 Column (75 μm × 50 cm, 2 μm, ThermoFisher, US)
138 with a linear gradient from 3% to 40% mobile phase B for 120 min at a flow rate of 300 nL/min

139 (mobile phase A: 1.95% ACN, 97.95% H_2O, 0.1% FA; mobile phase B: 79.95% ACN, 19.95%
140 H_2O, 0.1% FA). The mass spectrometer was operated in the data-dependent mode. A full-scan
141 survey MS experiment (m/z range from 375 to 2000; automatic gain control target, 1,000,000
142 ions; resolution at 400 m/z, 60,000; maximum ion accumulation time, 50 ms) was acquired by
143 the Orbitrap mass spectrometer, and ten most intense ions were fragmented by higher-energy C-
144 trap dissociation (HCD) with an optimized stepped collision energy (SCE) of 30 ± 15% NCE.

145 **Data analysis**

146 A modified version of pGlyco 2.0 was used to identify N-glycopeptides[27]. In the glycan
147 database, we defined an unnatural monosaccharide GalNAz (Gaz, Z). We created all the possible
148 "Gaz" containing human N-glycan sequences following the motif H(A)(Z), where "H" represents
149 Galactose, "A" represents Neu5Ac and "Z" represents GalNAz. For the sialoglycopeptides
150 identification, the raw data was first converted to an mgf file using pParse[46]. The potential
151 sialoglycopeptides spectra containing oxonium ions of both GlcNAc (m/z 204.09, m/z 186.08)
152 and Neu5Ac (m/z 292.10, m/z 274.09) were extracted and merged into a new mgf file using an
153 in-house program. The new mgf file was searched against an Uniprot-Swiss human protein
154 database (20,417 reviewed entries on March 20, 2019) and a modified N-glycan database. Other
155 searching parameters were used including carbamidomethyl (Cys) as a fixed modification,
156 deamination (Asn) and oxidation (Met) as variable modifications, and trypsin as the digestion
157 enzyme with maximum two missed cleavage sites allowed. The mass tolerance for the precursor
158 ions and the fragment ions was set to 10 ppm and 20 ppm, respectively. A total false discovery
159 rate (FDR) of 1% was applied to all data sets at the glycopeptide level. The identified
160 glycoproteins were annotated using Uniprot ID mapping[47].

161

162 **RESULTS AND DISCUSSION**

163 **The specificity of CgtA for Sialoglycopeptides**

164 Our previous study showed that CgtA had a high specificity for (Neu5Ac-α2,3-Gal)-
165 containing glycans[42]. To test its selectivity for sialoglycopeptides, we synthesized 23SP and
166 26SP (synthesis and data not published) as shown in **Figure 1A**. The activity of CgtA was
167 validated with sialolactose prior to the enzymatic reaction of sialoglycopeptides. After labeling
168 with GalNAz by CgtA, only α2,3-sialylated lactose showed a mass shift of 244 Da in the MS
169 spectrum and no substrate was obviously observed (**Figure S1**), which indicated that CgtA had
170 good catalytic activity and high specificity as well.

171 ESI-MS was used to monitor the GalNAz labeling reaction for sialoglycopeptides. For
172 the α2,3-sialoglycopeptide 23SP, the monoisotopic peak at m/z 1032.0808 is from the triply
173 charged glycopeptide (**Figure 1B**). After incubating with CgtA and UDP-GalNAz for 30 min, a
174 new dominant peak at m/z 1113.4422 with three positive charges was observed, which
175 correspond to the GalNAz labeled 23SP (**Figure 1D**). However, we could still detect minor
176 substrate 23SP. The α2,6-sialoglycopeptide 26SP has the same exact mass (**Figure 1C**) as 23SP.
177 After GalNAz labeling by CgtA, the strongest peak is located at the same exact position, and a
178 trace amount of product at m/z 1113.4422 was detected (**Figure 1E**). This may result from the
179 very weak activity of CgtA for 2,6-sialylated glycans[42].

180 The reaction time was further optimized to increase the conversion rate of GalNAz
181 labeling of 23SP. The reaction mixture at different time points was analyzed by LC-MS and the
182 reaction efficiency was calculated based on the peak area. For 23SP, in the first half an hour, the
183 reaction efficiency was dramatically increased. After that, the increase slowed down and the
184 reaction efficiency approached 100% at 60 min. Meanwhile, the conversion rate for the 26SP

185 remained unchanged (less than 1%) over time (**Figure 2**). Finally, we chose 60 min as the
186 reaction time for the subsequent GalNAz labeling reactions.
187
188 **Identifying Sialoglycopeptide Linkage Isomers by GalNAz Labeling and Tandem MS**
189 Although discrimination of α2,3/α2,6-sialoglycopeptide isomers can be achieved by the
190 mass shift in primary MS as shown above, we cannot accurately determine the glycopeptide
191 sequence using only molecular weight information. Tandem MS is an effective way for
192 sequencing glycopeptides, and HCD-MS/MS is commonly used to analyze glycopeptides
193 because of the high accuracy and detectable diagnostic oxonium ions of monosaccharides[26-28, 48].
194 It was also demonstrated that HCD with stepped collision energy (SCE) can simultaneously
195 determine the sequences of both glycans and peptides in a single run[27, 48]. To achieve a better
196 sequence coverage of glycopeptides on the Orbitrap we used, SCE was optimized with
197 glycopeptides enriched from human serum. The identification of N-glycopeptides was performed
198 using pGlyco 2.0 software[27]. A series of two-step SCEs and three-step SCEs were employed to
199 compare the number of identified glycopeptides. As shown in **Figure S2**, with a three-step SCE
200 of "15-30-45", more glycopeptides can be identified from the same sample.
201 The optimized SCE-HCD-MS/MS was applied for sequencing 23SP and 26SP. After
202 GalNAz labeling, 23SP (**Figure 3A**) showed diagnostic oxonium ions of GlcNAc and Neu5Ac at
203 m/z 204.09 and 292.10, which are common features of sialoglycopeptides. Apart from these
204 oxonium ions, 23SP also had a strong unknown peak at m/z 245.09. Compared with the spectrum
205 of 23SP before GalNAz labeling (**Figure S3**), we can obviously see that the peak with m/z
206 245.09 corresponds to the oxonium ion of GalNAz. Following the dissociation pathway of
207 GlcNAc[39, 49, 50] in **Scheme S1A**, a series of fragmentation ions of GalNAz in HCD were

208 illustrated in **Scheme S1B**. The peaks at m/z 245.09, m/z 227.08, m/z 209.07 and m/z 179.06,
209 which match the theoretical values very well, are diagnostic ions of GalNAz (**Figure S4**). For
210 26SP (**Figure 3B**), its spectrum showed that it shared similar fragmentation patterns with
211 GalNAz labeled 23SP. In the low m/z region, only diagnostic ions of GlcNAc and Neu5Ac were
212 observed, which clearly demonstrated that the GLAMS is an effective approach to distinguish
213 intact linkage specific sialoglycopeptides.
214
215 **Linkage Specific Sialoglycopeptides in Human Serum**
216 We then applied this method to analyze the N-linked α2,3/α2,6-sialoglycopeptides of
217 complex biological samples. Serum samples from healthy individuals (n = 4) and patients
218 diagnosed with liver cancer (n = 4) and colon cancer (n = 10) were used in this study. In the
219 beginning, we tried to perform the enzymatic labeling of the mixture of tryptic peptides and
220 glycopeptides. After drying from the FASP eluents, the mixture was not completely dissolved in
221 the Tris buffer (pH 7.5) for the enzymatic reaction, which may result from the existence of some
222 basic peptides. To solve the solubility issue, we adopted step-by-step glycopeptides enrichment
223 and enzymatic labeling as shown in the workflow **Figure 4**. It turned out that the enriched
224 glycopeptides were dissolved in the basic buffer very well. This may be attributed to that
225 conjugated glycans increase the hydrophilicity of peptides and some sialoglycans decrease the
226 isoelectric points of peptides according to the previous findings[51, 52].
227 All the serum samples were analyzed in three replicated LC-MS/MS runs for a large-
228 scale study of N-linked sialoglycopeptides. Using the oxonium ions of GalNAz as a tag to mark
229 α2,3-sialylation, a total of 18,822 sialoglycopeptide spectra were identified with a 1% total FDR,
230 corresponding to 1,138 unique site-specific sialoglycans on 220 N-glycosylation sites from 126

231 glycoproteins (**Table S1**), among of which 63% was also identified previously using a
232 deglycosylation method[53] as shown in **Figure S5**. For the distribution analysis of α2,3 or α2,6-
233 sialylation (**Figure 5A**), only 71 distinct site-specific sialoglycopeptides contained pure α2,3-
234 sialylation linkage, 186 sialoglycopeptides contained hybrid sialylation, and all the rest were
235 uniquely 2,6-sialylated, which accounts for more than 77% of the identified sialoglycopeptides.
236 This is consistent with the previous result that α2,6-sialylation is dominant in sialylated N-
237 glycans released from human serum samples[54]. Taking a closer look at the distribution of
238 sialylation levels, monosialylation is the major component in strictly α2,3 or α2,6-
239 sialoglycopeptides, and 83% of the hybrid sialoglycopeptides are disialylated.

240 The percentage of the overall overlapped glycosites (**Figure 5C**) and glycoproteins
241 (**Figure 5D**) in a specific type of serum is 76-84% and 75-80%, respectively. The percentage of
242 overlapping sialoglycopeptides (**Figure 5B**) in each kind of serum sample was significantly
243 lower than those of the glycosites and glycoproteins, reflecting the diversity of site-specific
244 glycosylation, especially for samples from colon cancer and liver cancer patients. A highly
245 glycosylated protein P01876 (IGHA1) was selected to demonstrate the diversity of site-specific
246 glycosylation in the three different sera. The previous study showed that IgA was α2,3 and α2,6-
247 sialylated on N-glycans[55]. Here, we identified 59 unique sialoglycopeptides including α2,3 and
248 α2,6 linkages on three known N-glycosylation sites of IGHA1 (**Table S1**). In addition, we found
249 some unique sialoglycopeptides of IGHA1 expressed in a serum-specific manner. For example,
250 both unique α2,6-sialoglycopeptides and hybrid sialoglycopeptides of IGHA1 were identified in
251 serum from colon cancer patients (representative spectra in **Figure S6**) and liver cancer patients
252 (representative spectra in **Figure S7**), whereas only one unique α2,6-sialoglycopeptide was
253 detected from control sera (**Figure S8**).

254 **CONCLUSIONS**

255 Elucidating linkage-specific sialylation of glycoproteins is significant to understand
256 pathogen-host interactions and disease development. By integrating enzymatic labeling and MS-
257 based glycoproteomics, we developed a high-throughput glycosyltransferase labeling assisted
258 mass spectrometry (GLAMS) to identify sialoglycopeptide linkage isomers. Facilitated by the
259 acceptor specificity of the glycosyltransferase CgtA toward the Neu5Ac(α2,3)Gal epitope, we
260 have demonstrated the distinct diagnostic oxonium ions as tags to effectively discriminate α2,3-
261 and α2,6-sialoglycopeptide isomers using LC separation coupled with SCE-HCD-MS/MS
262 fragmentation. We also successfully applied this approach to a large-scale profiling of linkage-
263 specific sialoglycopeptides in human serum samples. The strategy of GLAMS should be of great
264 benefit in investigating differential changes in response to disease states from a glycoproteomics
265 perspective, and has potential to contribute to biomarker discovery in many diseases.

266

267

268

269

270

271

272

273

274

275

276

AUTHOR INFORMATION

Corresponding Authors

lli22@gsu.edu (L. L.) or pwang11@gsu.edu (P. G. W.)

Author Contributions

H.Z., L. L., and P. G. W. conceived the project; H.Z. designed and performed the experiments, analyzed the data, and wrote the manuscript; S. W. synthesized the sialoglycopeptides; D. L. and L. D. prepared the serum glycopeptides for collision energy optimization; C. C., Y. L. and Z. W. synthesized the UDP-GalNAz; R. B. and K. L. collected and prepared the human serum samples; C. M., J. Y., L. L., and P. G. W. edited the manuscript. All the authors revised and approved the manuscript.

ACKNOWLEDGEMENTS

We sincerely thank Dr. Wenfeng Zeng from the Key Lab of Intelligent Information Processing of Chinese Academy of Sciences for the help of parameter setting of pGlyco 2.0, Georgia Cancer Center Biorepository for providing human serum samples, and Georgia Research Alliance for financial support to purchase mass spectrometers. This work is supported by National Institute of Health (U01GM116263 and U54HL142019).

CONFLICT OF INTERESTS

The authors declare no conflict of interest.

300 **REFERENCES**

301 1. Ohtsubo, K.; Marth, J. D., Glycosylation in cellular mechanisms of health and disease.
302 *Cell* **2006,** *126* (5), 855-67.
303 2. Banerjee, S.; Vishwanath, P.; Cui, J.; Kelleher, D. J.; Gilmore, R.; Robbins, P. W.;
304 Samuelson, J., The evolution of N-glycan-dependent endoplasmic reticulum quality control
305 factors for glycoprotein folding and degradation. *P Natl Acad Sci USA* **2007,** *104* (28), 11676-
306 11681.
307 3. Furukawa, K.; Ohkawa, Y.; Yamauchi, Y.; Hamamura, K.; Ohmi, Y.; Furukawa, K.,
308 Fine tuning of cell signals by glycosylation. *J Biochem* **2012,** *151* (6), 573-578.
309 4. Rudd, P. M.; Elliott, T.; Cresswell, P.; Wilson, I. A.; Dwek, R. A., Glycosylation and
310 the immune system. *Science* **2001,** *291* (5512), 2370-2376.
311 5. Karlsson, K. A., Pathogen-host protein-carbohydrate interactions as the basis of
312 important infections. *Adv Exp Med Biol* **2001,** *491*, 431-443.
313 6. Apweiler, R.; Hermjakob, H.; Sharon, N., On the frequency of protein glycosylation, as
314 deduced from analysis of the SWISS-PROT database. *Bba-Gen Subjects* **1999,** *1473* (1), 4-8.
315 7. Zielinska, D. F.; Gnad, F.; Wisniewski, J. R.; Mann, M., Precision Mapping of an In
316 Vivo N-Glycoproteome Reveals Rigid Topological and Sequence Constraints. *Cell* **2010,** *141* (5),
317 897-907.
318 8. Varki, N. M.; Varki, A., Diversity in cell surface sialic acid presentations: implications
319 for biology and disease. *Lab Invest* **2007,** *87* (9), 851-7.
320 9. Varki, A.; Schauer, R., Sialic Acids. In *Essentials of Glycobiology*, nd; Varki, A.;
321 Cummings, R. D.; Esko, J. D.; Freeze, H. H.; Stanley, P.; Bertozzi, C. R.; Hart, G. W.; Etzler,
322 M. E., Eds. Cold Spring Harbor (NY), 2009.
323 10. Stevens, J.; Blixt, O.; Paulson, J. C.; Wilson, I. A., Glycan microarray technologies:
324 tools to survey host specificity of influenza viruses. *Nat Rev Microbiol* **2006,** *4* (11), 857-64.
325 11. Hatakeyama, S.; Yoneyama, T.; Tobisawa, Y.; Ohyama, C., Recent progress and
326 perspectives on prostate cancer biomarkers. *Int J Clin Oncol* **2017,** *22* (2), 214-221.
327 12. Mancera-Arteu, M.; Gimenez, E.; Barbosa, J.; Sanz-Nebot, V., Identification and
328 characterization of isomeric N-glycans of human alfa-acid-glycoprotein by stable isotope
329 labelling and ZIC-HILIC-MS in combination with exoglycosidase digestion. *Anal Chim Acta*
330 **2016,** *940*, 92-103.
331 13. Mechref, Y.; Kang, P.; Novotny, M. V., Differentiating structural isomers of sialylated
332 glycans by matrix-assisted laser desorption/ionization time-of-flight/time-of-flight tandem mass
333 spectrometry. *Rapid Commun Mass Sp* **2006,** *20* (8), 1381-1389.
334 14. Alley, W. R., Jr.; Novotny, M. V., Glycomic analysis of sialic acid linkages in glycans
335 derived from blood serum glycoproteins. *J Proteome Res* **2010,** *9* (6), 3062-72.
336 15. Jiang, K.; Zhu, H.; Li, L.; Guo, Y. X.; Gashash, E.; Ma, C.; Sun, X. L.; Li, J.; Zhang,
337 L. W.; Wang, P. G., Sialic acid linkage-specific permethylation for improved profiling of protein
338 glycosylation by MALDI-TOF MS. *Anal Chim Acta* **2017,** *981*, 53-61.
339 16. Wheeler, S. F.; Domann, P.; Harvey, D. J., Derivatization of sialic acids for stabilization
340 in matrix-assisted laser desorption/ionization mass spectrometry and concomitant differentiation
341 of α(2→3) and α(2→6)-isomers. *Rapid Commun Mass Spectrom* **2009,** *23* (2), 303-12.
342 17. Reiding, K. R.; Blank, D.; Kuijper, D. M.; Deelder, A. M.; Wuhrer, M., High-
343 Throughput Profiling of Protein N-Glycosylation by MALDI-TOF-MS Employing Linkage-
344 Specific Sialic Acid Esterification. *Anal Chem* **2014,** *86* (12), 5784-5793.

18. Holst, S.; Heijs, B.; de Haan, N.; van Zeijl, R. J. M.; Briaire-de Bruijn, I. H.; van Pelt, G. W.; Mehta, A. S.; Angel, P. M.; Mesker, W. E.; Tollenaar, R. A.; Drake, R. R.; Bovee, J. V. M. G.; McDonnell, L. A.; Wuhrer, M., Linkage-Specific in Situ Sialic Acid Derivatization for N-Glycan Mass Spectrometry Imaging of Formalin-Fixed Paraffin-Embedded Tissues. *Anal Chem* **2016,** *88* (11), 5904-5913.
19. Yang, S.; Jankowska, E.; Kosikova, M.; Xie, H.; Cipollo, J., Solid-Phase Chemical Modification for Sialic Acid Linkage Analysis: Application to Glycoproteins of Host Cells Used in Influenza Virus Propagation. *Anal Chem* **2017,** *89* (17), 9508-9517.
20. Li, H. H.; Gao, W. J.; Feng, X. J.; Liu, B. F.; Liu, X., MALDI-MS analysis of sialylated N-glycan linkage isomers using solid-phase two step derivatization method. *Anal Chim Acta* **2016,** *924*, 77-85.
21. Nishikaze, T.; Tsurnoto, H.; Sekiya, S.; Iwamoto, S.; Miura, Y.; Tanaka, K., Differentiation of Sialyl Linkage Isomers by One-Pot Sialic Acid Derivatization for Mass Spectrometry-Based Glycan Profiling. *Anal Chem* **2017,** *89* (4), 2353-2360.
22. Chen, C. H.; Lin, Y. P.; Lin, J. L.; Li, S. T.; Ren, C. T.; Wu, C. Y.; Chen, C. H., Rapid Identification of Terminal Sialic Acid Linkage Isomers by Pseudo-MS3 Mass Spectrometry. *Isr J Chem* **2015,** *55* (3-4), 412-422.
23. Guttman, M.; Lee, K. K., Site-Specific Mapping of Sialic Acid Linkage Isomers by Ion Mobility Spectrometry. *Anal Chem* **2016,** *88* (10), 5212-5217.
24. Depland, A. D.; Renois-Predelus, G.; Schindler, B.; Compagnon, I., Identification of sialic acid linkage isomers in glycans using coupled InfraRed Multiple Photon Dissociation (IRMPD) spectroscopy and mass spectrometry. *Int J Mass Spectrom* **2018,** *434*, 65-69.
25. Woo, C. M.; Iavarone, A. T.; Spiciarich, D. R.; Palaniappan, K. K.; Bertozzi, C. R., Isotope-targeted glycoproteomics (IsoTaG): a mass-independent platform for intact N- and O-glycopeptide discovery and analysis. *Nat Methods* **2015,** *12* (6), 561-7.
26. Sun, S. S.; Shah, P.; Eshghi, S. T.; Yang, W. M.; Trikannad, N.; Yang, S.; Chen, L. J.; Aiyetan, P.; Hoti, N.; Zhang, Z.; Chan, D. W.; Zhang, H., Comprehensive analysis of protein glycosylation by solid-phase extraction of N-linked glycans and glycosite-containing peptides. *Nat Biotechnol* **2016,** *34* (1), 84-88.
27. Liu, M. Q.; Zeng, W. F.; Fang, P.; Cao, W. Q.; Liu, C.; Yan, G. Q.; Zhang, Y.; Peng, C.; Wu, J. Q.; Zhang, X. J.; Tu, H. J.; Chi, H.; Sun, R. X.; Cao, Y.; Dong, M. Q.; Jiang, B. Y.; Huang, J. M.; Shen, H. L.; Wong, C. C. L.; He, S. M.; Yang, P. Y., pGlyco 2.0 enables precision N-glycoproteomics with comprehensive quality control and one-step mass spectrometry for intact glycopeptide identification. *Nat Commun* **2017,** *8*.
28. Stadlmann, J.; Taubenschmid, J.; Wenzel, D.; Gattinger, A.; Durnberger, G.; Dusberger, F.; Elling, U.; Mach, L.; Mechtler, K.; Penninger, J. M., Comparative glycoproteomics of stem cells identifies new players in ricin toxicity. *Nature* **2017,** *549* (7673), 538-+.
29. Riley, N. M.; Hebert, A. S.; Westphall, M. S.; Coon, J. J., Capturing site-specific heterogeneity with large-scale N-glycoproteome analysis. *Nat Commun* **2019,** *10*.
30. Nishikaze, T.; Nakamura, T.; Jinmei, H.; Amano, J., Negative-ion MALDI-MS2 for discrimination of alpha2,3- and alpha2,6-sialylation on glycopeptides labeled with a pyrene derivative. *J Chromatogr B Analyt Technol Biomed Life Sci* **2011,** *879* (17-18), 1419-28.
31. de Haan, N.; Reiding, K. R.; Haberger, M.; Reusch, D.; Falck, D.; Wuhrer, M., Linkage-Specific Sialic Acid Derivatization for MALDI-TOF-MS Profiling of IgG Glycopeptides. *Anal Chem* **2015,** *87* (16), 8284-8291.

391 32. Yang, S.; Wu, W. W.; Shen, R. F.; Bern, M.; Cipollo, J., Identification of Sialic Acid
392 Linkages on Intact Glycopeptides via Differential Chemical Modification Using IntactGIG-
393 HILIC. *J Am Soc Mass Spectr* **2018,** *29* (6), 1273-1283.
394 33. Hinneburg, H.; Hofmann, J.; Struwe, W. B.; Thader, A.; Altmann, F.; Silva, D. V.;
395 Seeberger, P. H.; Pagel, K.; Kolarich, D., Distinguishing N-acetylneuraminic acid linkage
396 isomers on glycopeptides by ion mobility-mass spectrometry. *Chem Commun* **2016,** *52* (23),
397 4381-4384.
398 34. Pett, C.; Nasir, W.; Sihlbom, C.; Olsson, B. M.; Caixeta, V.; Schorlemer, M.; Zahedi,
399 R. P.; Larson, G.; Nilsson, J.; Westerlind, U., Effective Assignment of alpha 2,3/alpha 2,6-
400 Sialic Acid Isomers by LC-MS/MS-Based Glycoproteomics. *Angew Chem Int Edit* **2018,** *57* (30),
401 9320-9324.
402 35. Khidekel, N.; Arndt, S.; Lamarre-Vincent, N.; Lippert, A.; Poulin-Kerstien, K. G.;
403 Ramakrishnan, B.; Qasba, P. K.; Hsieh-Wilson, L. C., A chemoenzymatic approach toward the
404 rapid and sensitive detection of O-GlcNAc posttranslational modifications. *J Am Chem Soc* **2003,**
405 *125* (52), 16162-3.
406 36. Chaubard, J. L.; Krishnamurthy, C.; Yi, W.; Smith, D. F.; Hsieh-Wilson, L. C.,
407 Chemoenzymatic probes for detecting and imaging fucose-alpha(1-2)-galactose glycan
408 biomarkers. *J Am Chem Soc* **2012,** *134* (10), 4489-92.
409 37. Mbua, N. E.; Li, X.; Flanagan-Steet, H. R.; Meng, L.; Aoki, K.; Moremen, K. W.;
410 Wolfert, M. A.; Steet, R.; Boons, G. J., Selective exo-enzymatic labeling of N-glycans on the
411 surface of living cells by recombinant ST6Gal I. *Angew Chem Int Ed Engl* **2013,** *52* (49), 13012-
412 5.
413 38. Li, Q.; Li, Z.; Duan, X.; Yi, W., A tandem enzymatic approach for detecting and
414 imaging tumor-associated Thomsen-Friedenreich antigen disaccharide. *J Am Chem Soc* **2014,**
415 *136* (36), 12536-9.
416 39. Zheng, J.; Xiao, H.; Wu, R., Specific Identification of Glycoproteins Bearing the Tn
417 Antigen in Human Cells. *Angew Chem Int Ed Engl* **2017,** *56* (25), 7107-7111.
418 40. Wen, L.; Liu, D.; Zheng, Y.; Huang, K.; Cao, X.; Song, J.; Wang, P. G., A One-Step
419 Chemoenzymatic Labeling Strategy for Probing Sialylated Thomsen-Friedenreich Antigen. *ACS*
420 *Cent Sci* **2018,** *4* (4), 451-457.
421 41. Wu, Z. L. L.; Person, A. D.; Anderson, M.; Burroughs, B.; Tatge, T.; Khatri, K.; Zou,
422 Y. L.; Wang, L. C.; Geders, T.; Zaia, J.; Sackstein, R., Imaging specific cellular glycan
423 structures using glycosyltransferases via click chemistry. *Glycobiology* **2018,** *28* (2), 69-79.
424 42. Wen, L. Q.; Zheng, Y.; Jiang, K.; Zhang, M. Z.; Kondengaden, S. M.; Li, S. S.;
425 Huang, K.; Li, J.; Song, J.; Wang, P. G., Two-Step Chemoenzymatic Detection of N-
426 Acetylneuraminic Acid-alpha(2-3)-Galactose Glycans. *J Am Chem Soc* **2016,** *138* (36), 11473-
427 11476.
428 43. Wu, Z.; Liu, Y.; Ma, C.; Li, L.; Bai, J.; Byrd-Leotis, L.; Lasanajak, Y.; Guo, Y.;
429 Wen, L.; Zhu, H.; Song, J.; Li, Y.; Steinhauer, D. A.; Smith, D. F.; Zhao, B.; Chen, X.;
430 Guan, W.; Wang, P. G., Identification of the binding roles of terminal and internal glycan
431 epitopes using enzymatically synthesized N-glycans containing tandem epitopes. *Org Biomol*
432 *Chem* **2016,** *14* (47), 11106-11116.
433 44. Wisniewski, J. R.; Zougman, A.; Nagaraj, N.; Mann, M., Universal sample preparation
434 method for proteome analysis. *Nat Methods* **2009,** *6* (5), 359-62.

435 45. Parker, B. L.; Thaysen-Andersen, M.; Solis, N.; Scott, N. E.; Larsen, M. R.; Graham,
436 M. E.; Packer, N. H.; Cordwell, S. J., Site-specific glycan-peptide analysis for determination of
437 N-glycoproteome heterogeneity. *J Proteome Res* **2013,** *12* (12), 5791-800.
438 46. Yuan, Z. F.; Liu, C.; Wang, H. P.; Sun, R. X.; Fu, Y.; Zhang, J. F.; Wang, L. H.; Chi,
439 H.; Li, Y.; Xiu, L. Y.; Wang, W. P.; He, S. M., pParse: a method for accurate determination of
440 monoisotopic peaks in high-resolution mass spectra. *Proteomics* **2012,** *12* (2), 226-35.
441 47. UniProt, C., The Universal Protein Resource (UniProt). *Nucleic Acids Res* **2007,** *35*
442 (Database issue), D193-7.
443 48. Pioch, M.; Hoffmann, M.; Pralow, A.; Reichl, U.; Rapp, E., glyXtool(MS): An Open-
444 Source Pipeline for Semiautomated Analysis of Glycopeptide Mass Spectrometry Data. *Anal*
445 *Chem* **2018,** *90* (20), 11908-11916.
446 49. Zhao, P.; Viner, R.; Teo, C. F.; Boons, G. J.; Horn, D.; Wells, L., Combining high-
447 energy C-trap dissociation and electron transfer dissociation for protein O-GlcNAc modification
448 site assignment. *J Proteome Res* **2011,** *10* (9), 4088-104.
449 50. Halim, A.; Westerlind, U.; Pett, C.; Schorlemer, M.; Ruetschi, U.; Brinkmalm, G.;
450 Sihlbom, C.; Lengqvist, J.; Larson, G.; Nilsson, J., Assignment of saccharide identities through
451 analysis of oxonium ion fragmentation profiles in LC-MS/MS of glycopeptides. *J Proteome Res*
452 **2014,** *13* (12), 6024-32.
453 51. Willey, K. P., An elusive role for glycosylation in the structure and function of
454 reproductive hormones. *Hum Reprod Update* **1999,** *5* (4), 330-55.
455 52. Hayakawa, S.; Nakai, S., Relationships of Hydrophobicity and Net Charge to the
456 Solubility of Milk and Soy Proteins. *Journal of Food Science* **1985,** *50* (2), 486-491.
457 53. Zhu, H.; Li, X.; Qu, J.; Xiao, C.; Jiang, K.; Gashash, E.; Liu, D.; Song, J.; Cheng, J.;
458 Ma, C.; Wang, P. G., Diethylaminoethyl Sepharose (DEAE-Sepharose) microcolumn for
459 enrichment of glycopeptides. *Anal Bioanal Chem* **2017,** *409* (2), 511-518.
460 54. Jiang, K.; Zhu, H.; Li, L.; Guo, Y.; Gashash, E.; Ma, C.; Sun, X.; Li, J.; Zhang, L.;
461 Wang, P. G., Sialic acid linkage-specific permethylation for improved profiling of protein
462 glycosylation by MALDI-TOF MS. *Anal Chim Acta* **2017,** *981*, 53-61.
463 55. Maurer, M. A.; Meyer, L.; Bianchi, M.; Turner, H. L.; Le, N. P. L.; Steck, M.;
464 Wyrzucki, A.; Orlowski, V.; Ward, A. B.; Crispin, M.; Hangartner, L., Glycosylation of
465 Human IgA Directly Inhibits Influenza A and Other Sialic-Acid-Binding Viruses. *Cell Rep* **2018,**
466 *23* (1), 90-99.
467

468

469

470

471

472 **Captions for Figures, Tables and Schemes**

473

474 **Scheme 1**. Strategy for distinguishing α2,3/α2,6-sialoglycopeptides by glycosyltransferase
475 labeling assisted mass spectrometry.

476

477 **Figure 1**. (A) Structure of the synthesized α2,3-sialoglycopeptides (23SP) and α2,6-
478 sialoglycopeptides (26SP); ESI-MS spectra of 23SP (B) and 26SP (C) before enzymatic labeling,
479 and 23SP (D) and 26SP (E) after enzymatic labeling.

480

481 **Figure 2**. Time optimization for CgtA labeling of 23SP and 26SP.

482

483 **Figure 3**. HCD-MS/MS spectra of 23SP (A) and 26SP (B) after enzymatic labeling.

484

485 **Figure 4**. Workflow for identification of linkage specific sialoglycopeptides from human serum.

486

487 **Figure 5**. (A) Distribution of the sialoglycopeptides from human serum; Venn diagrams of
488 identified glycopeptides (B), N-glycosylation sites (C), and glycoproteins (D) in serum samples
489 from colon cancer patients, liver cancer patients and normal people.

490

491 **Figure S1**. MALDI-MS spectra of 6SL (A) and 3SL (C) before enzymatic labeling and 6SL (B)
492 and 3SL (D) after enzymatic labeling.

493

494 **Figure S2**. Identification number of N-glycopeptides in normal human serum under different
495 collision energies.

496 **Figure S3**. Tandem MS spectrum of 23SP with HCD fragmentation before enzymatic labeling.

497

498 **Scheme S1**. Dissociation pathways for the GlcNAc (A) and GalNAz (B) in HCD mode.

499

500 **Figure S4**. Zoomed-in spectra of 23SP before enzymatic labeling (A) and 23SP after enzymatic
501 labeling (B).

502

503 **Figure S5**. Venn diagram of identified glycoproteins from current study and previous study in
504 which deglycosylation method was used.
505
506 **Figure S6**. Representative annotated spectra of α2,6-sialylated glycopeptide (top) and α2,3-
507 sialylated glycopeptide (bottom) in the protein P01876 from colon cancer patients' serum. Green
508 circles indicate Hexose, blue squares indicate GlcNAc, olive squares represent GalNAz, purple
509 diamonds indicate Neu5Ac, and red triangles indicate Fuc.
510
511 **Figure S7**. Representative annotated spectra of α2,6-sialylated glycopeptide (top) and α2,3-
512 sialylated glycopeptide (bottom) in the protein P01876 from liver cancer patients' serum.
513
514 **Figure S8**. Representative annotated spectrum of α2,6-sialylated glycopeptide in the protein
515 P01876 from normal human sera.
516
517 **Table S1.** Identified N-glycosite-specific sialoglycans in serum samples from cancer patients and
518 normal people. SC: serum for colon cancer patients; SL: serum from liver cancer patients; SN:
519 serum from normal people. "X" indicates detected glycopeptides in a specific sample; "H"
520 indicates Hexose; "N" indicates GlcNAc; "A" indicates Neu5Ac; "Z" indicates GalNAz; "F"
521 indicates Fuc.

Abstract

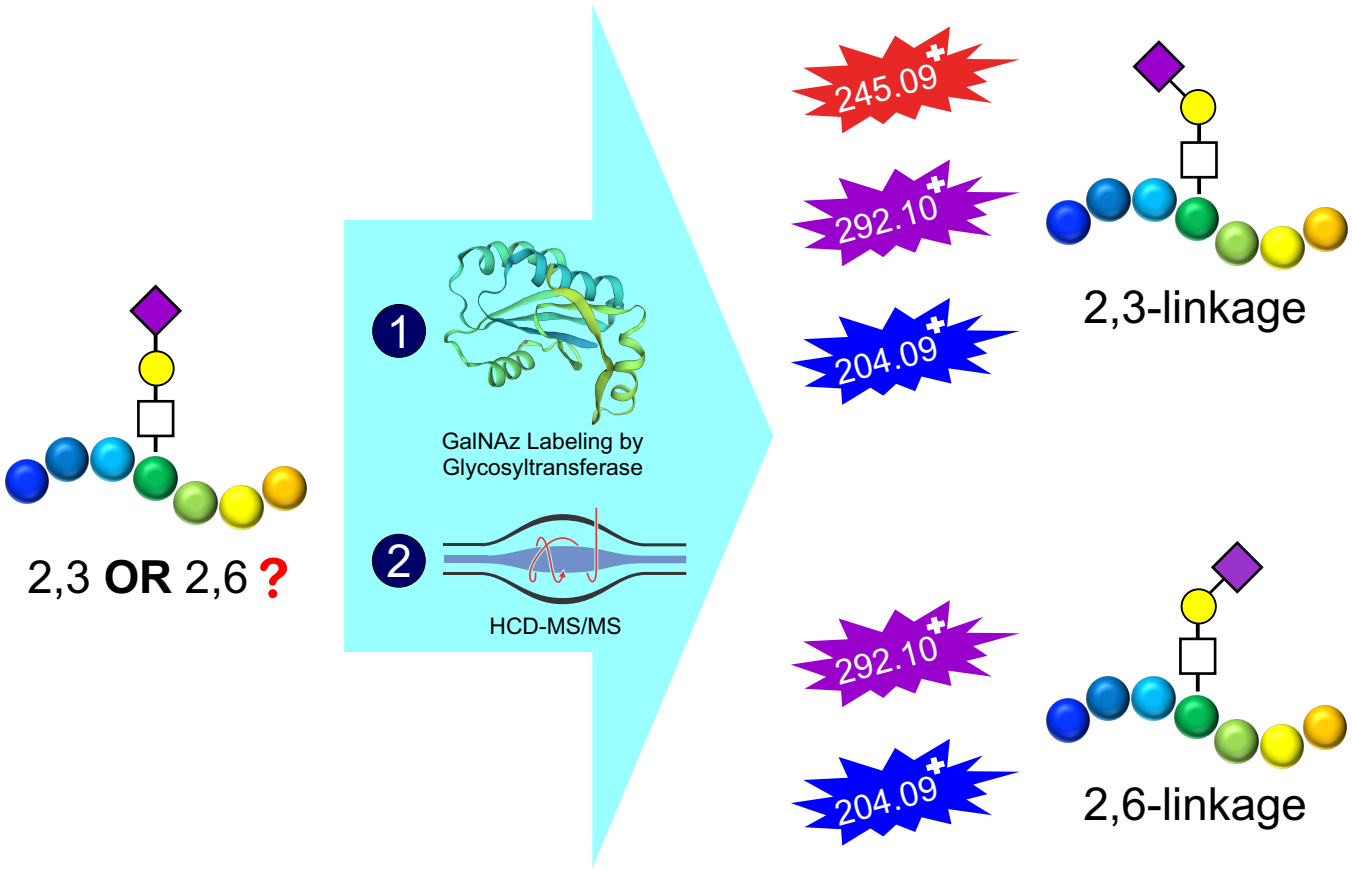
2,3 OR 2,6 ?
1
GalNAz Labeling by
Glycosyltransferase
2
HCD-MS/MS
245.09+
292.10+
204.09+
2,3-linkage
292.10+
204.09+
2,6-linkage

Scheme 1

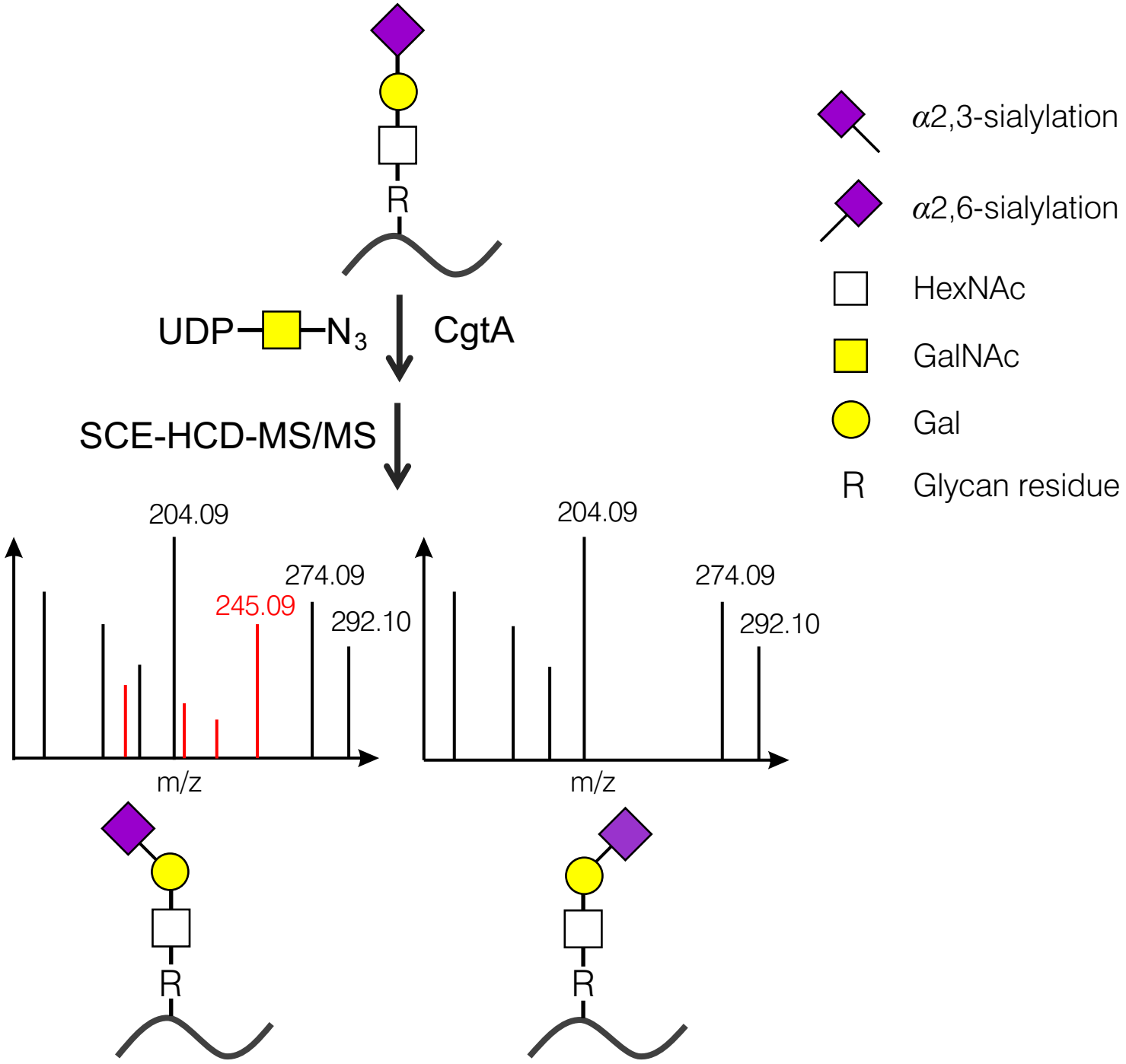
R
UDP
N3
CgtA
SCE-HCD-MS/MS
204.09
274.09
245.09
292.10
m/z
204.09
274.09
292.10
m/z
R
R
α2,3-sialylation
α2,6-sialylation
HexNAc
GalNAc
Gal
R
Glycan residue

Figure 1

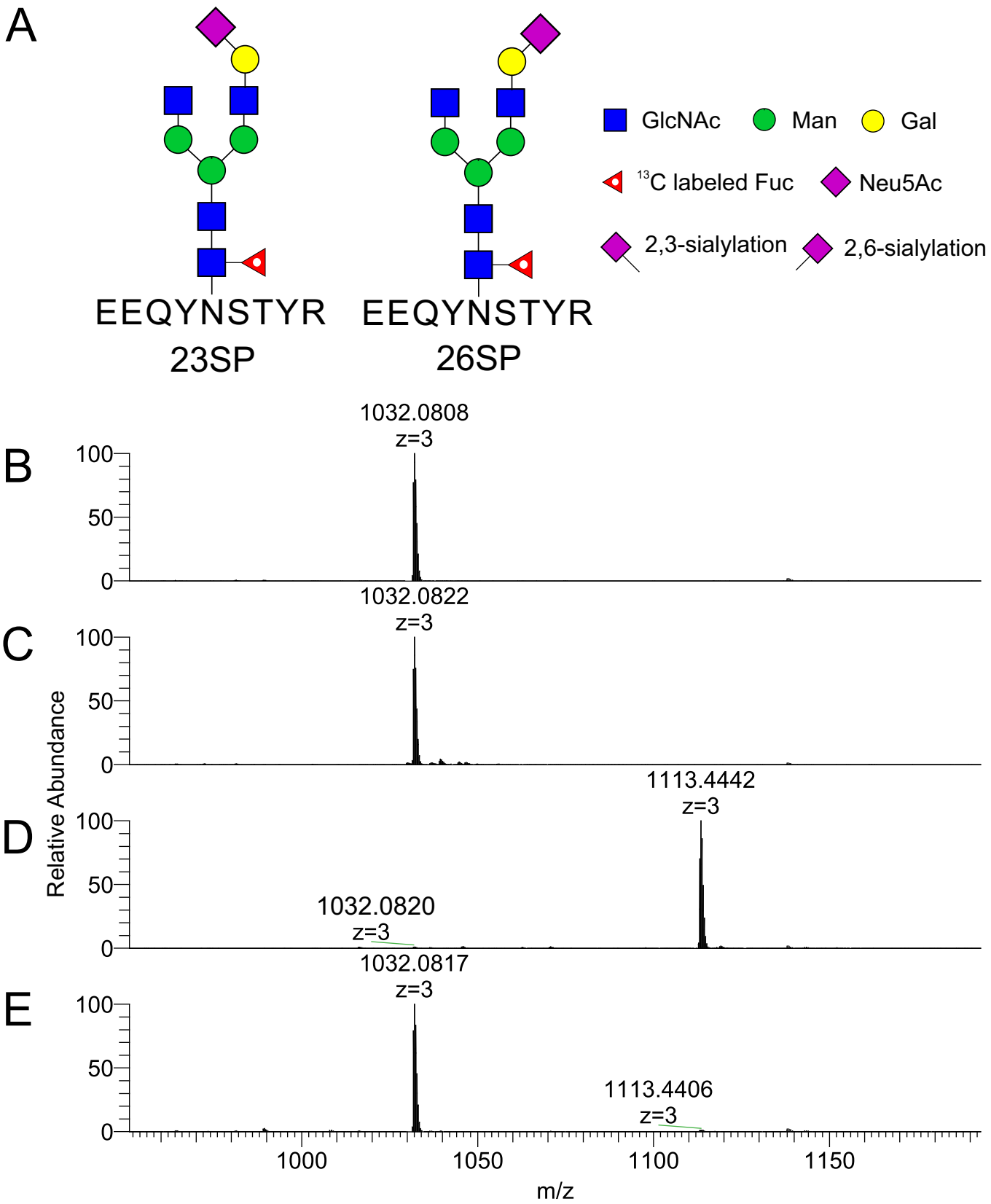
A
EEQYNSTYR
23SP
EEQYNSTYR
26SP
GlcNAc
Man
Gal
13C labeled Fuc
Neu5Ac
2,3-sialylation
2,6-sialylation
B
1032.0808
z=3
C
1032.0822
z=3
D
1113.4442
z=3
1032.0820
z=3
E
1032.0817
z=3
1113.4406
z=3
Relative Abundance
100
50
0
1000
1050
1100
1150
m/z

Figure 2

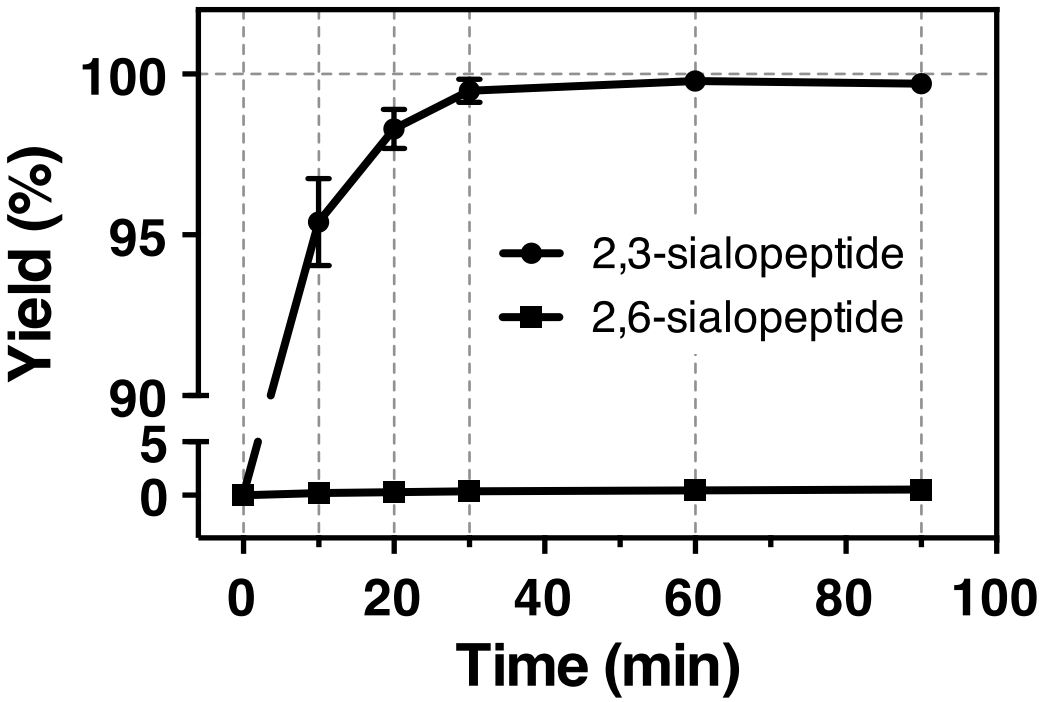
100
95
90
5
0
Yield (%)
2,3-sialopeptide
2,6-sialopeptide
0
20
40
60
80
100
Time (min)

Figure 3

A

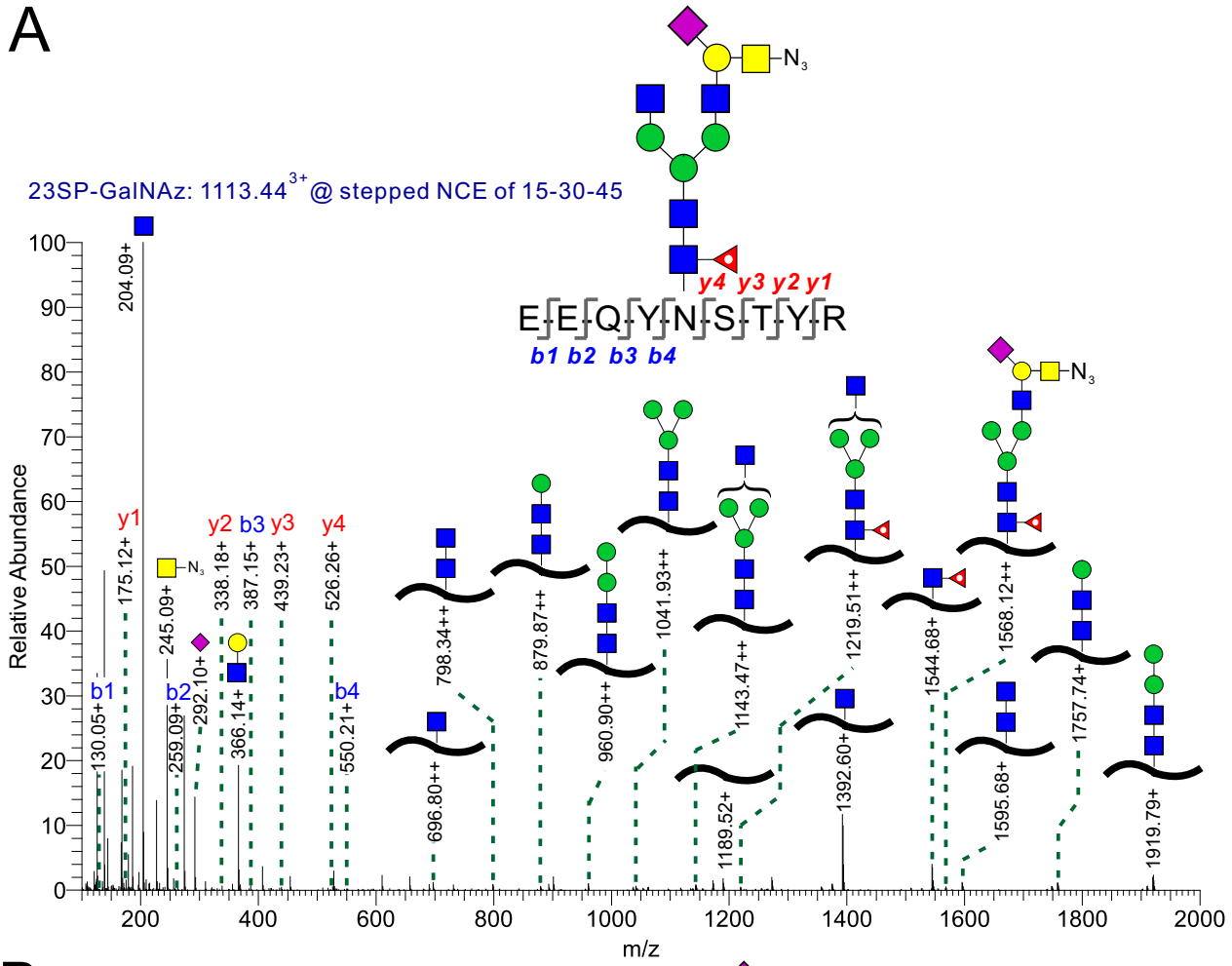
23SP-GalNAz: 1113.44 3+ @ stepped NCE of 15-30-45
N3
y4 y3 y2 y1
E-E-Q-Y-N-S-T-Y-R
b1 b2 b3 b4
Relative Abundance
m/z
204.09+
y1
175.12+
245.09+
y2 b3 y3
338.18+
387.15+
439.23+
y4
526.26+
b1
130.05+
b2
259.09+
292.10+
366.14+
b4
550.21+
798.34++
879.87++
960.90++
1041.93++
1143.47++
1219.51++
1544.68+
1568.12++
1757.74+
1919.79+
696.80++
1189.52+
1392.60+
1595.68+

B

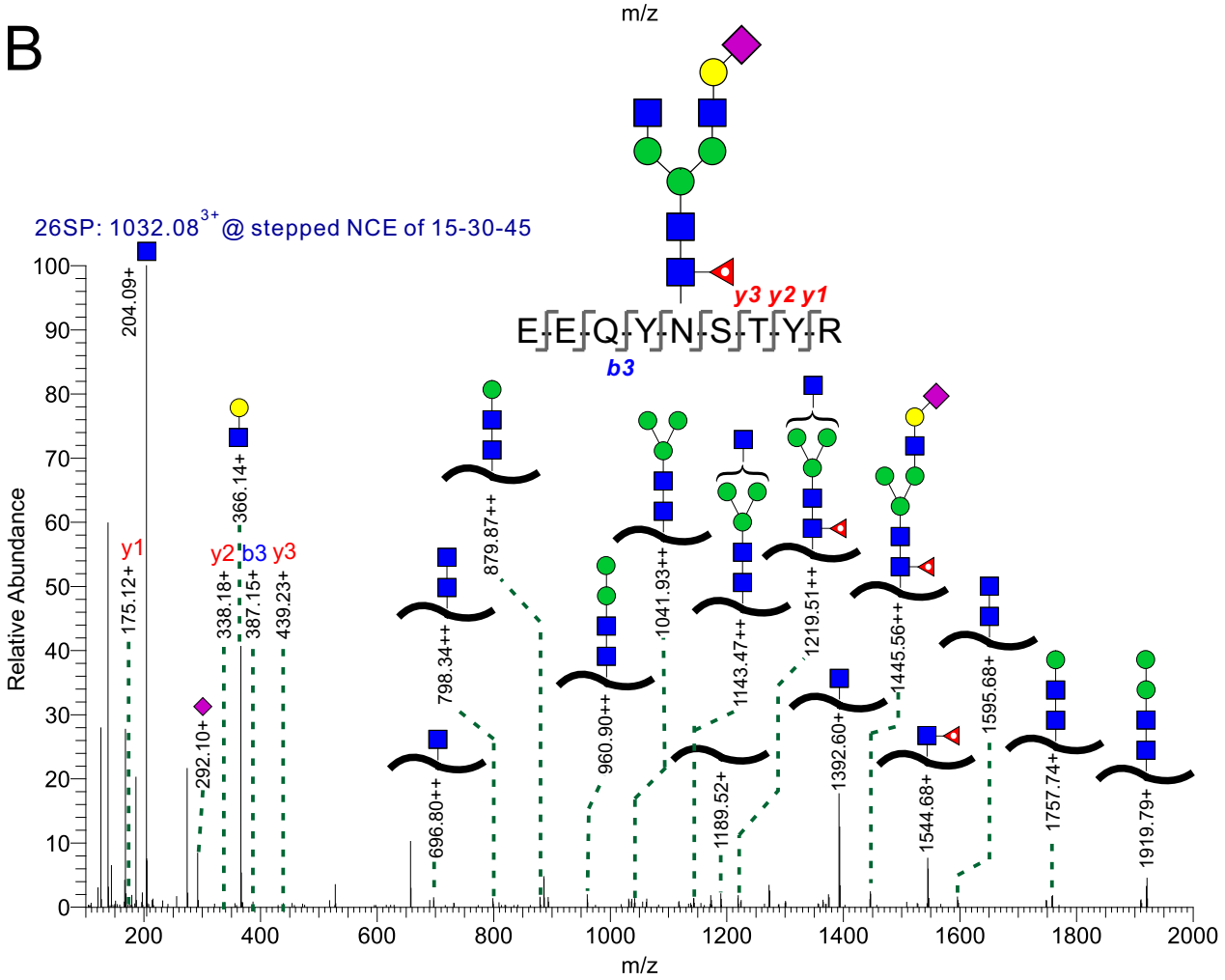
26SP: 1032.08 3+ @ stepped NCE of 15-30-45
y3 y2 y1
E-E-Q-Y-N-S-T-Y-R
b3
Relative Abundance
m/z
204.09+
y1
175.12+
292.10+
y2 b3 y3
338.18+
366.14+
387.15+
439.23+
798.34++
879.87++
960.90++
1041.93++
1143.47++
1219.51++
1445.56++
1544.68+
1595.68+
1757.74+
1919.79+
696.80++
1189.52+
1392.60+

Figure 4

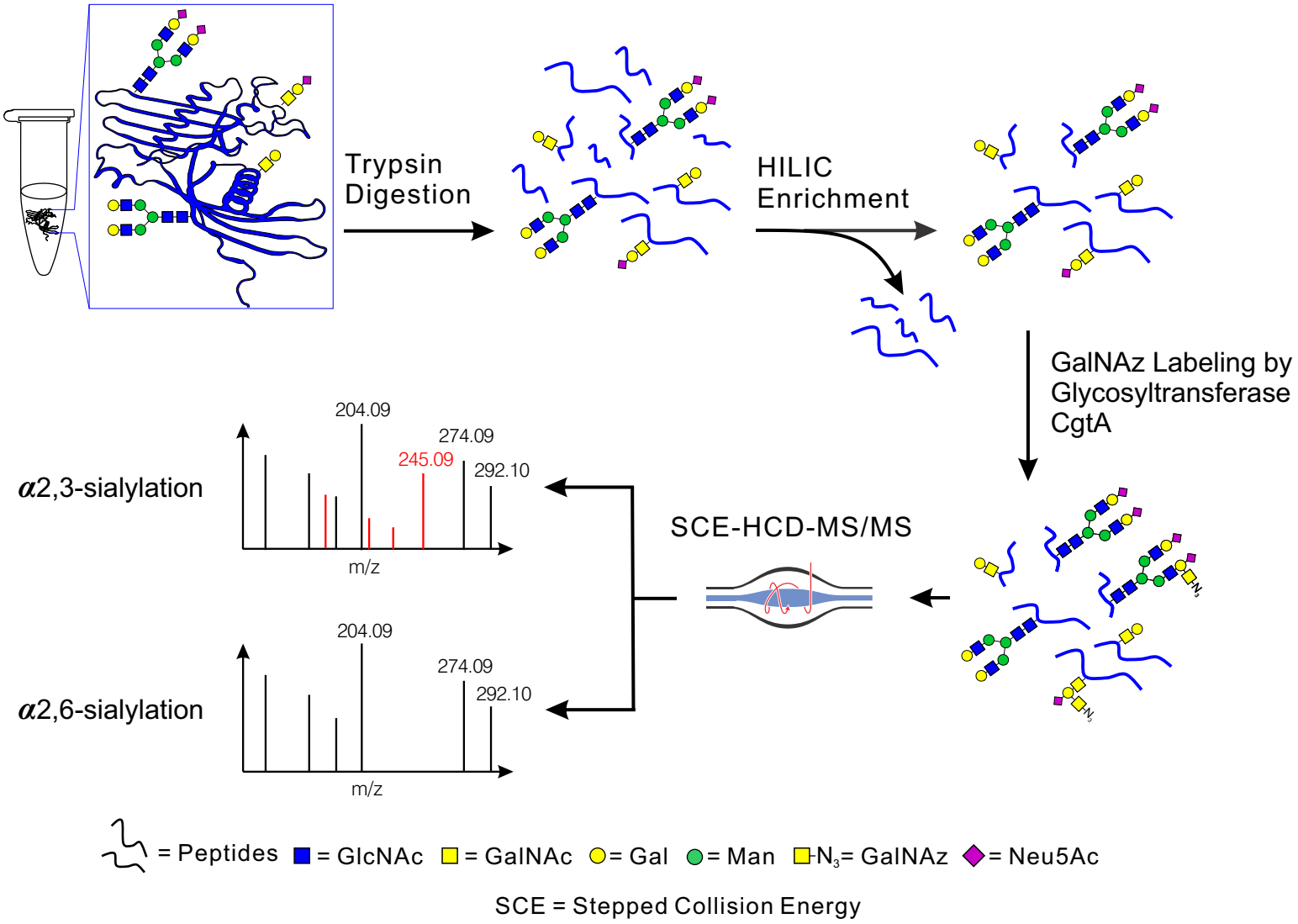
Trypsin
Digestion
HILIC
Enrichment
GalNAz Labeling by
Glycosyltransferase
CgtA
SCE-HCD-MS/MS
α2,3-sialylation
204.09
274.09
245.09
292.10
m/z
α2,6-sialylation
204.09
274.09
292.10
m/z
= Peptides
= GlcNAc
= GalNAc
= Gal
= Man
-N3= GalNAz
= Neu5Ac
SCE = Stepped Collision Energy

Figure 5

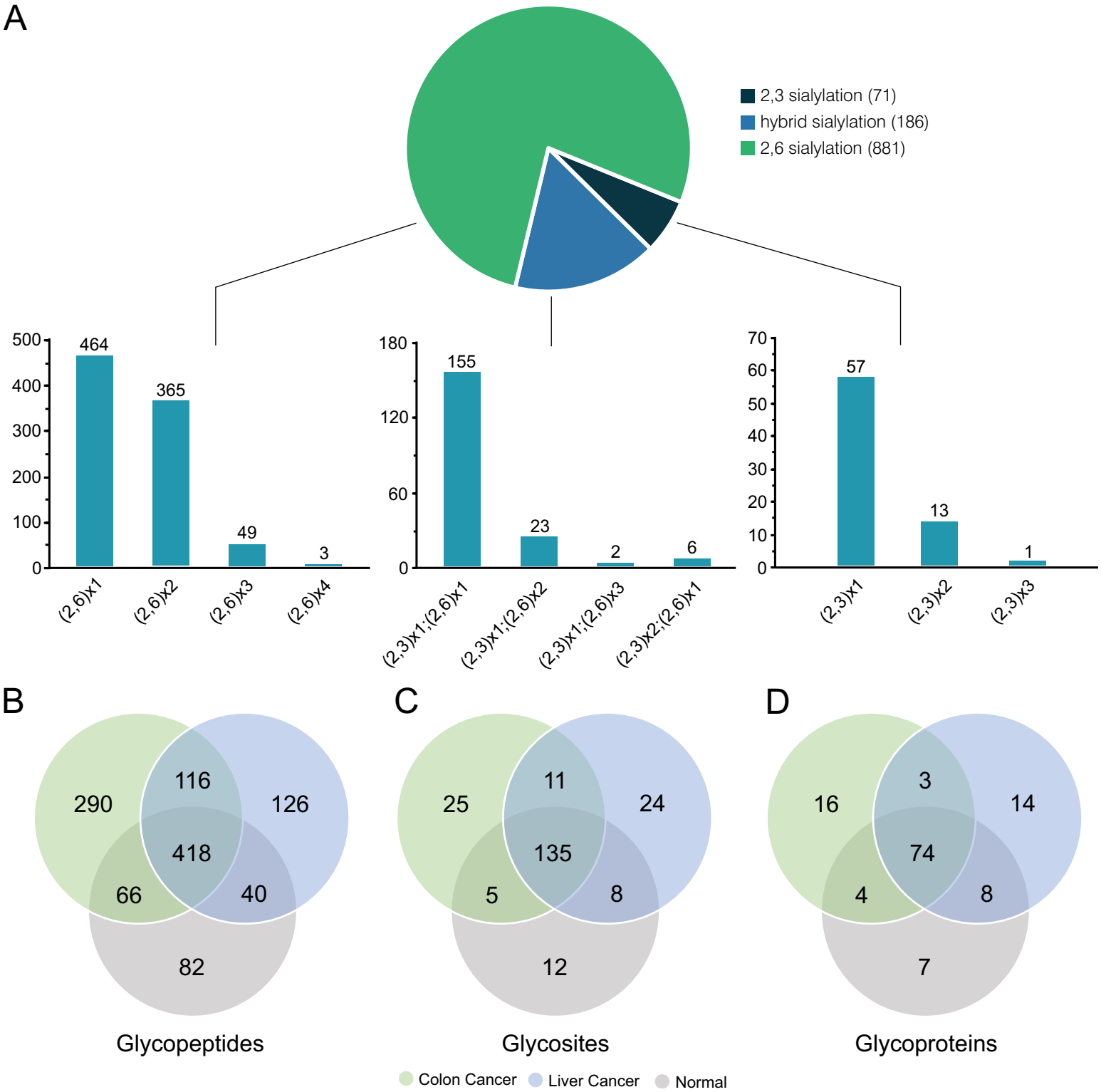
A
2,3 sialylation (71)
hybrid sialylation (186)
2,6 sialylation (881)
464
365
49
3
(2,6)x1
(2,6)x2
(2,6)x3
(2,6)x4
155
23
2
6
(2,3)x1;(2,6)x1
(2,3)x1;(2,6)x2
(2,3)x1;(2,6)x3
(2,3)x2;(2,6)x1
57
13
1
(2,3)x1
(2,3)x2
(2,3)x3
B
290
116
126
418
66
40
82
Glycopeptides
C
25
11
24
135
5
8
12
Glycosites
D
16
3
14
74
4
8
7
Glycoproteins
Colon Cancer
Liver Cancer
Normal

Figure S1

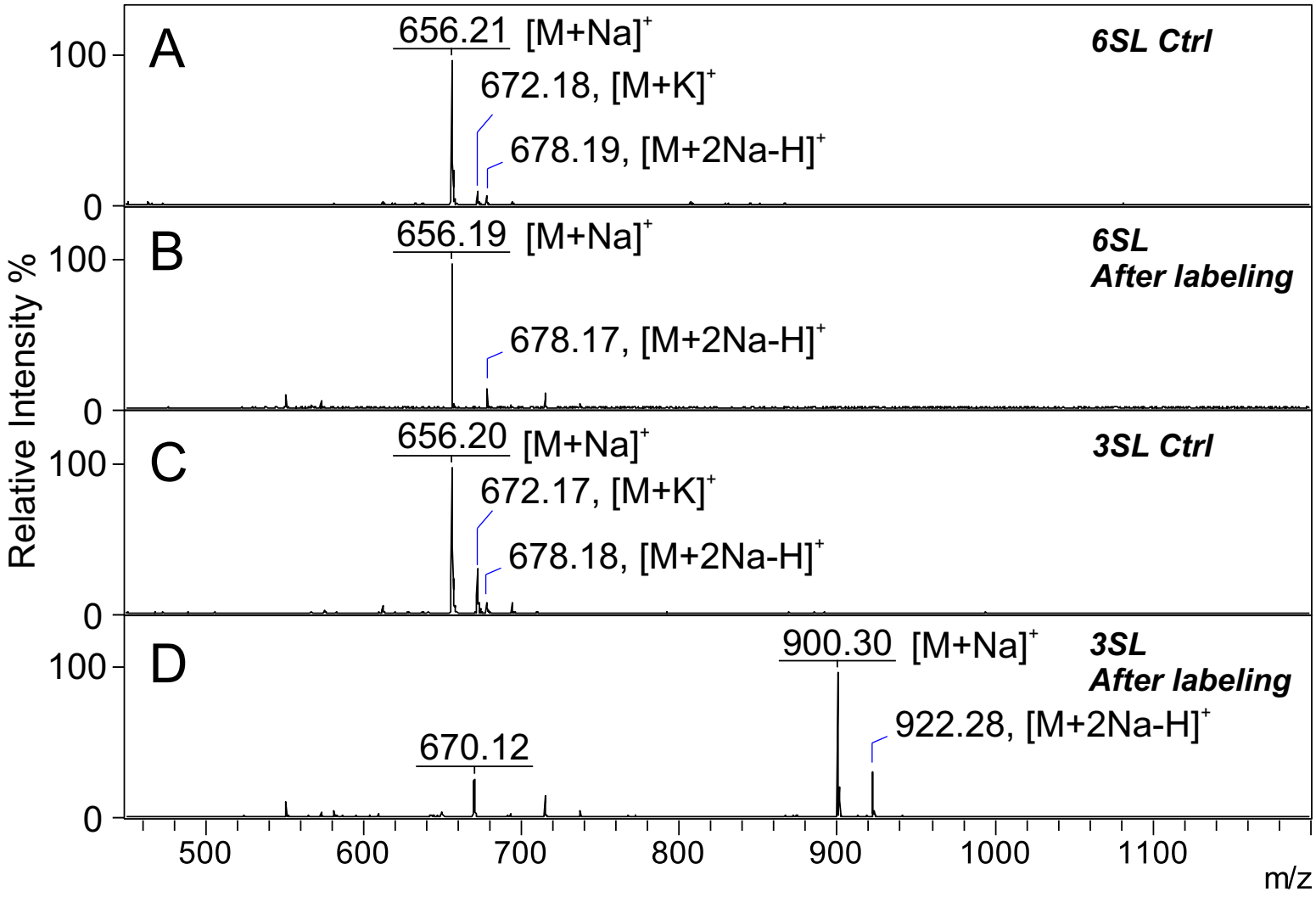
A
656.21 [M+Na]+
672.18, [M+K]+
678.19, [M+2Na-H]+
6SL Ctrl
B
656.19 [M+Na]+
678.17, [M+2Na-H]+
6SL
After labeling
C
656.20 [M+Na]+
672.17, [M+K]+
678.18, [M+2Na-H]+
3SL Ctrl
D
900.30 [M+Na]+
922.28, [M+2Na-H]+
670.12
3SL
After labeling
Relative Intensity %
100
0
500
600
700
800
900
1000
1100
m/z

Figure S2

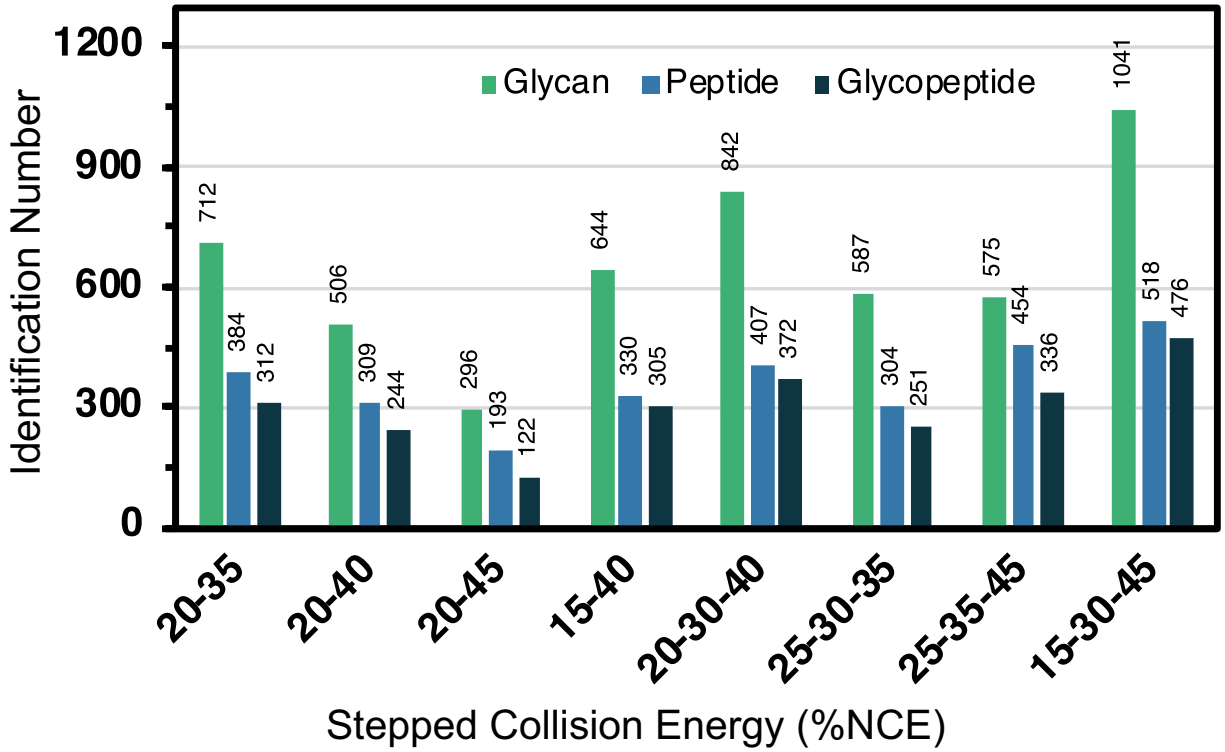
Glycan
Peptide
Glycopeptide
Identification Number
1200
900
600
300
0
712
384
312
506
309
244
296
193
122
644
330
305
842
407
372
587
304
251
575
454
336
1041
518
476
20-35
20-40
20-45
15-40
20-30-40
25-30-35
25-35-45
15-30-45
Stepped Collision Energy (%NCE)

Figure S3

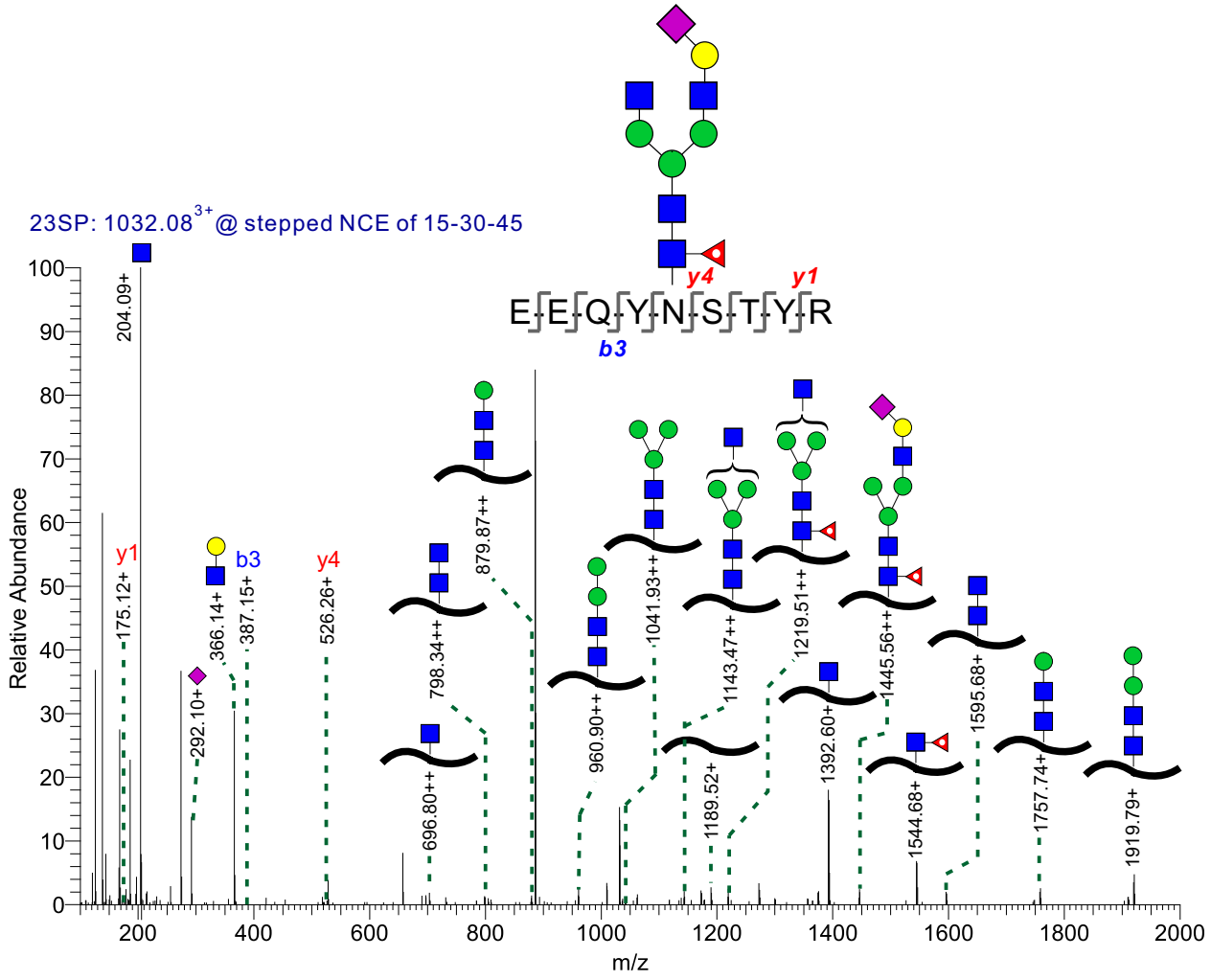
23SP: 1032.08 3+ @ stepped NCE of 15-30-45
E-E-Q-Y-N-S-T-Y-R
y4
y1
b3
Relative Abundance
m/z
204.09+
175.12+
292.10+
366.14+
387.15+
526.26+
696.80++
798.34++
879.87++
960.90++
1041.93++
1143.47++
1189.52+
1219.51++
1392.60+
1445.56++
1544.68+
1595.68+
1757.74+
1919.79+

Scheme S1

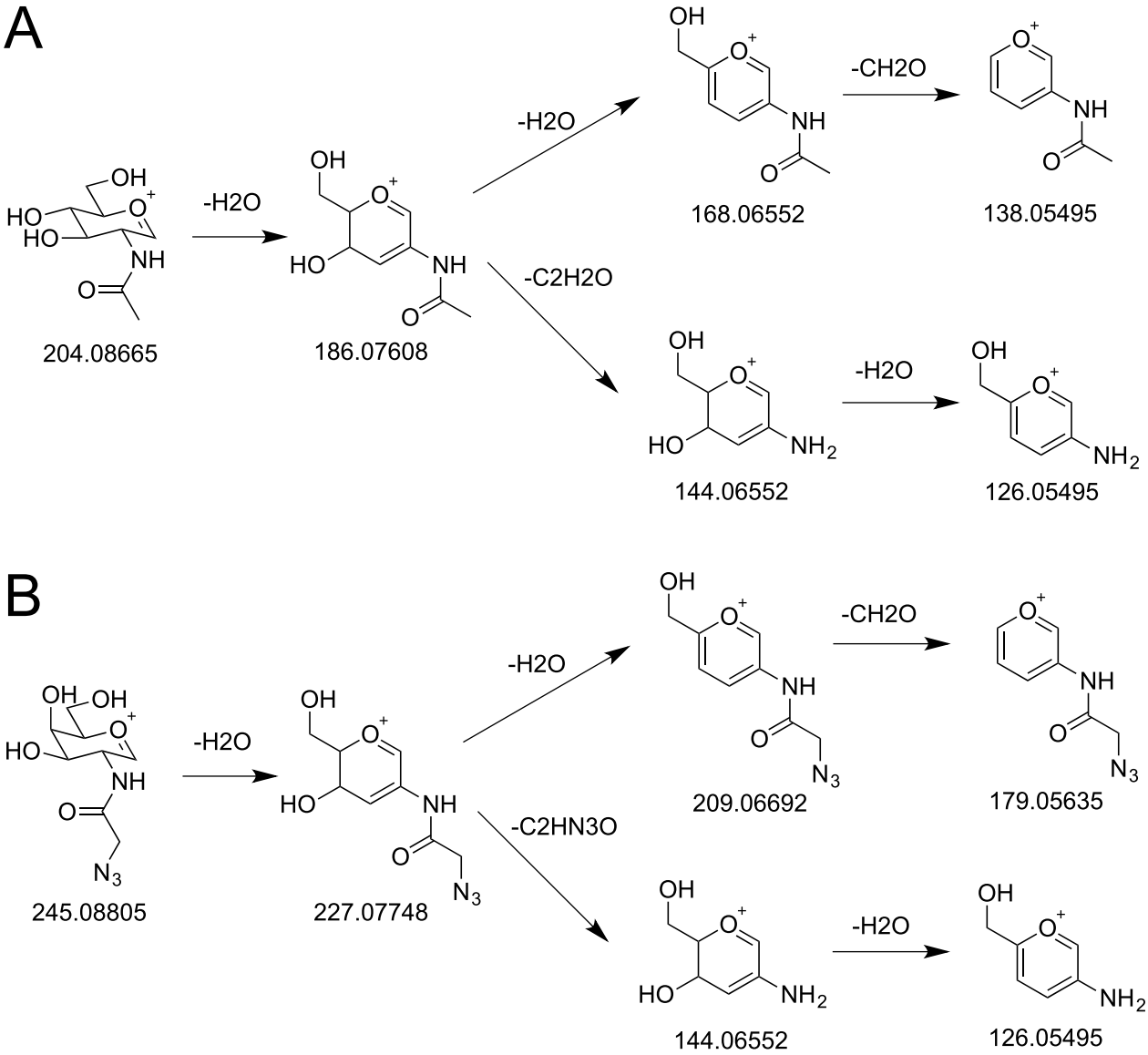
A
-H2O
-H2O
-C2H2O
-CH2O
-H2O
204.08665
186.07608
168.06552
138.05495
144.06552
126.05495
B
-H2O
-H2O
-C2HN3O
-CH2O
-H2O
245.08805
227.07748
209.06692
179.05635
144.06552
126.05495

Figure S4

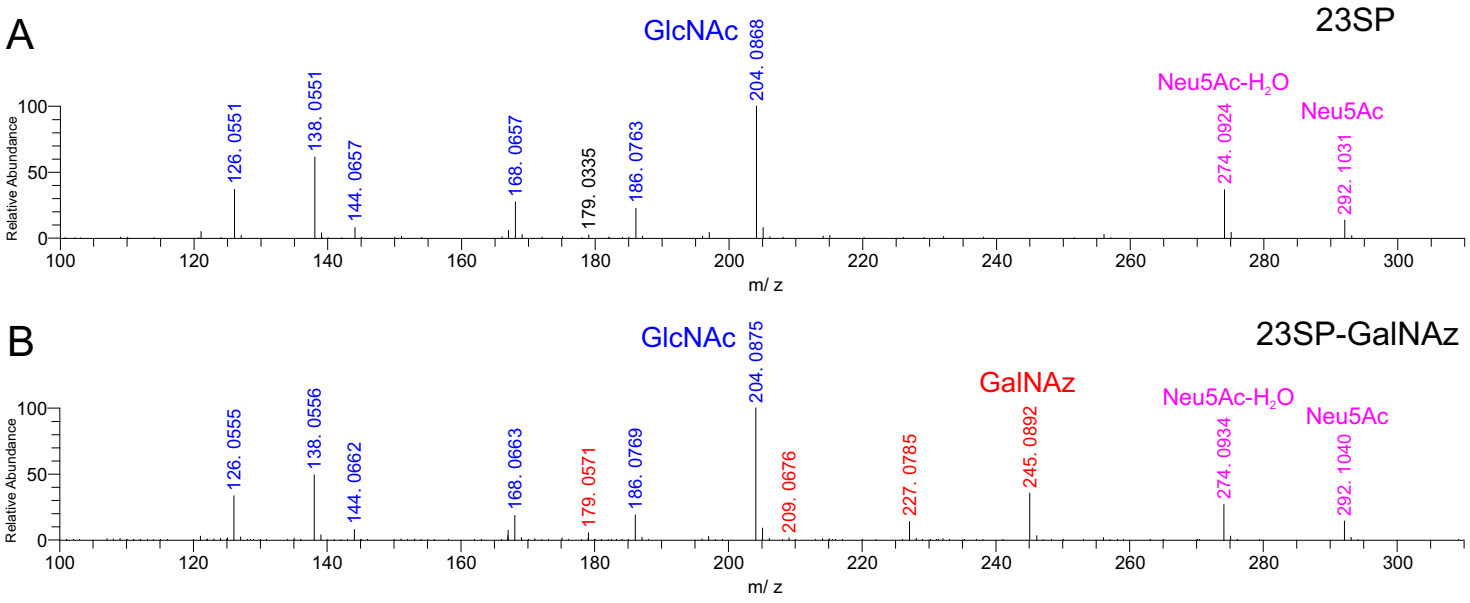
A
23SP
GlcNAc
204. 0868
Neu5Ac-H2O
Neu5Ac
126. 0551
138. 0551
144. 0657
168. 0657
179. 0335
186. 0763
274. 0924
292. 1031
Relative Abundance
m/ z

B
23SP-GalNAz
GlcNAc
204. 0875
GalNAz
Neu5Ac-H2O
Neu5Ac
126. 0555
138. 0556
144. 0662
168. 0663
179. 0571
186. 0769
209. 0676
227. 0785
245. 0892
274. 0934
292. 1040
Relative Abundance
m/ z

Figure S5

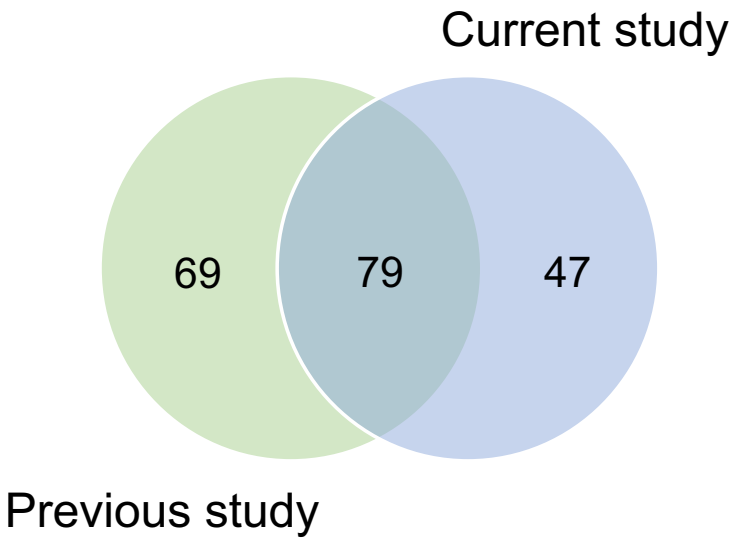

Figure S6

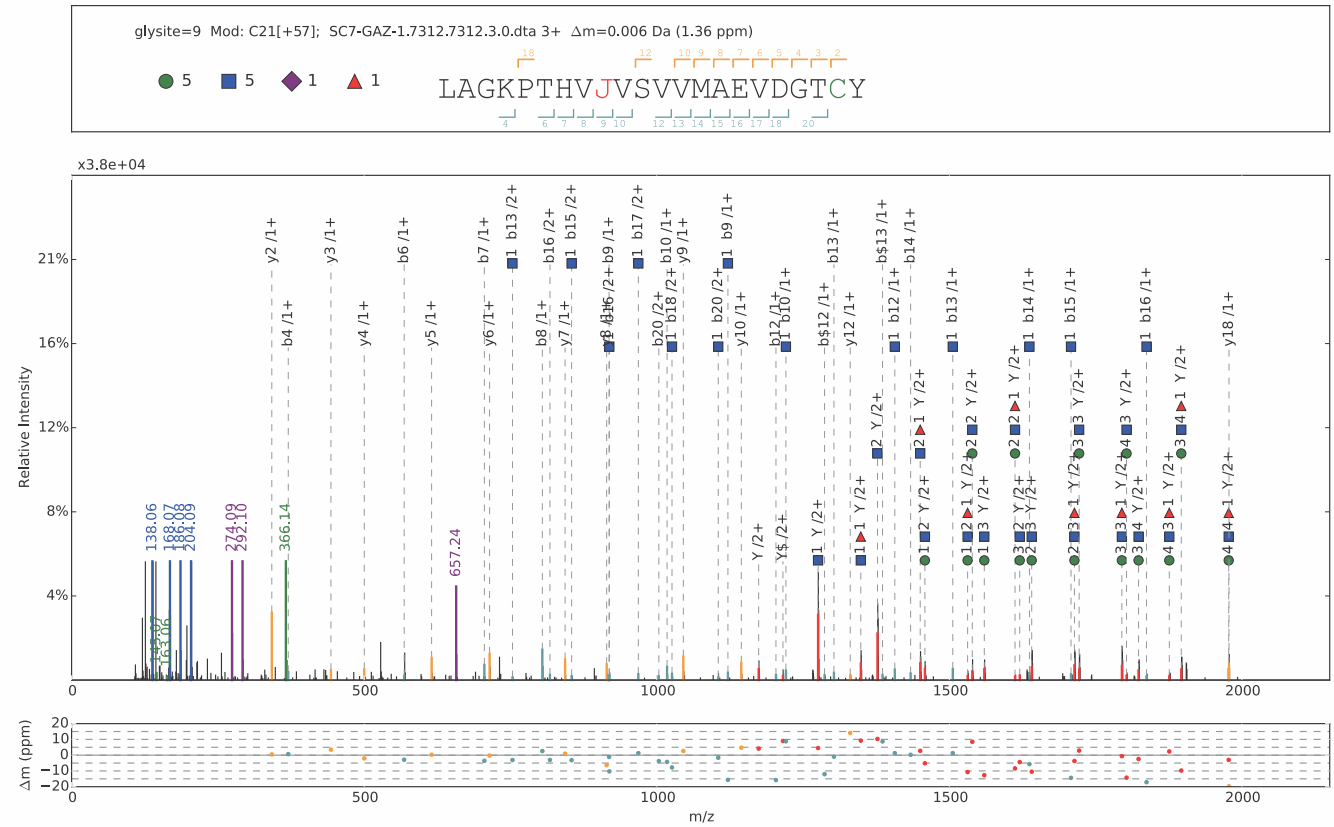
glysite=9 Mod: C21[+57]; SC7-GAZ-1.7312.7312.3.0.dta 3+ Δm=0.006 Da (1.36 ppm)
LAGKPTHVJVSVVMAEVDGTCY
x3.8e+04
Relative Intensity
Δm (ppm)
m/z

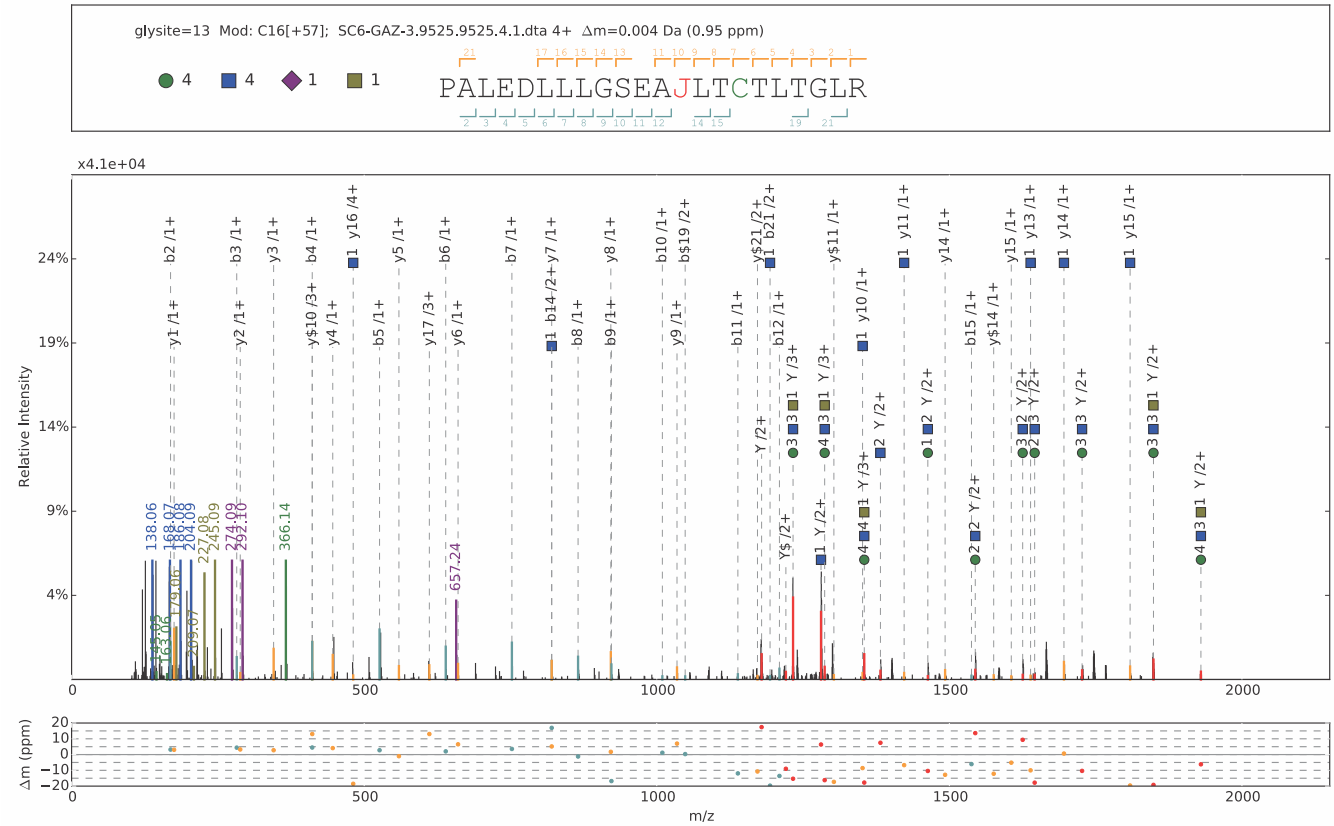
glysite=13 Mod: C16[+57]; SC6-GAZ-3.9525.9525.4.1.dta 4+ Δm=0.004 Da (0.95 ppm)
PALEDLLLGSEAJLTCTLTGLR
x4.1e+04
Relative Intensity
Δm (ppm)
m/z

Figure S7

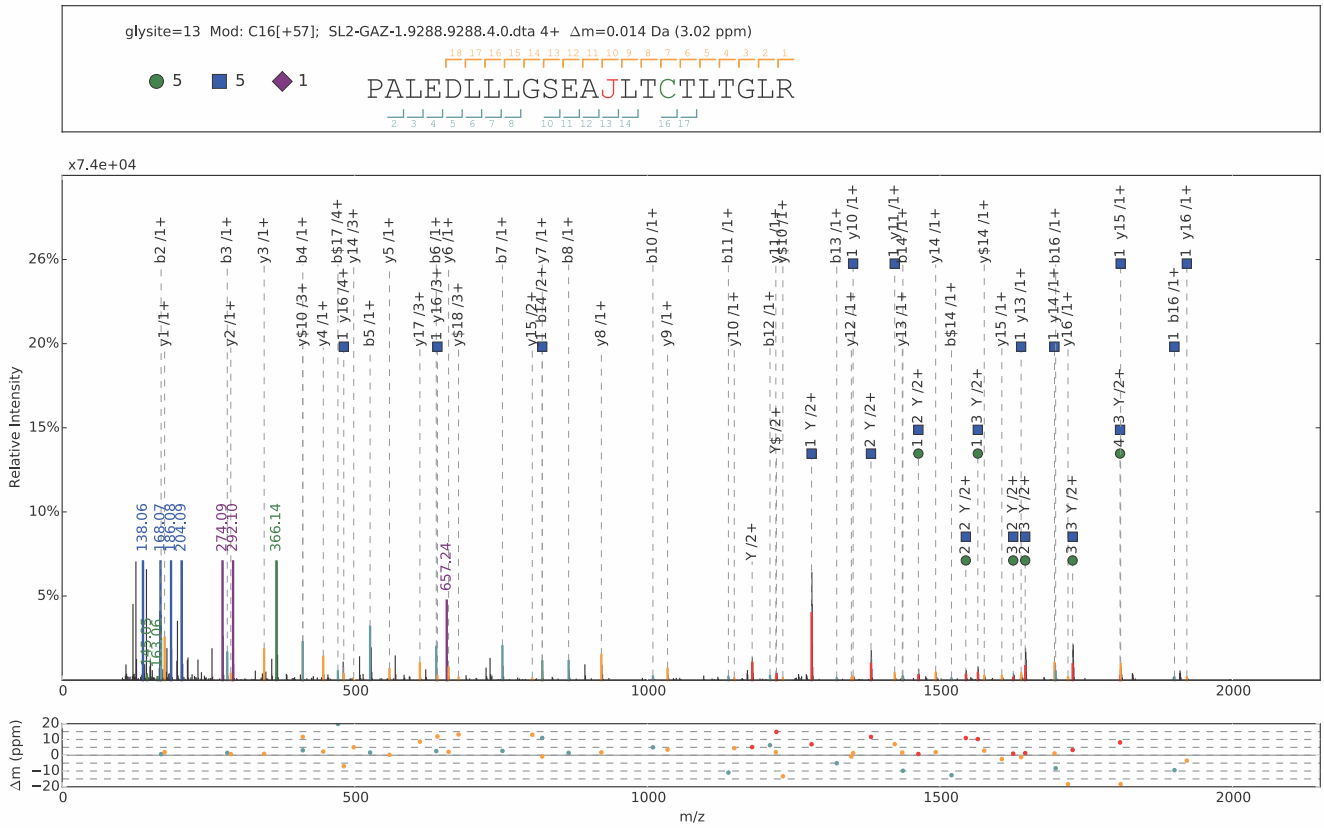
glysite=13 Mod: C16[+57]; SL2-GAZ-1.9288.9288.4.0.dta 4+ Δm=0.014 Da (3.02 ppm)
5 5 1
PALEDLLLGSEAJLTCTLTGLR
x7.4e+04
Relative Intensity
Δm (ppm)
m/z

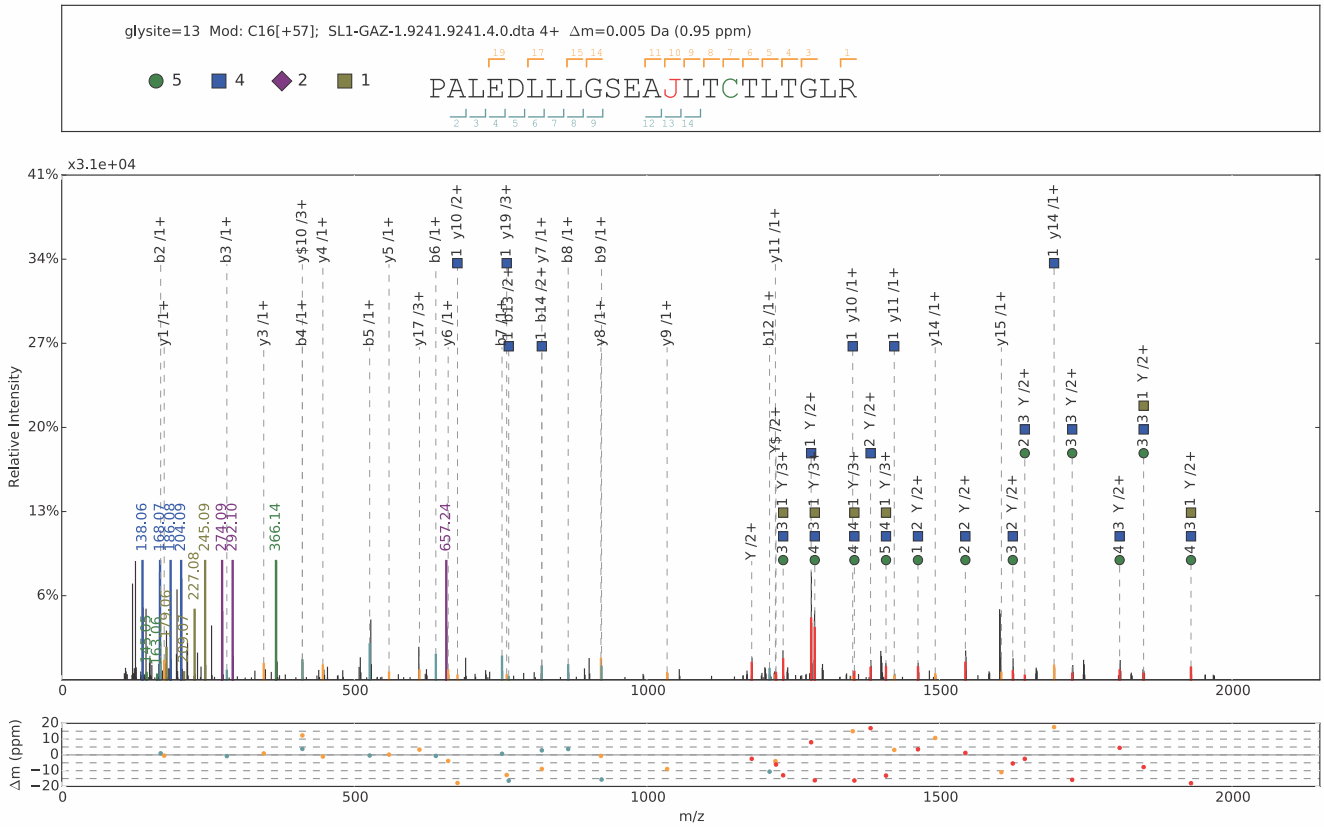
glysite=13 Mod: C16[+57]; SL1-GAZ-1.9241.9241.4.0.dta 4+ Δm=0.005 Da (0.95 ppm)
5 4 2 1
PALEDLLLGSEAJLTCTLTGLR
x3.1e+04
Relative Intensity
Δm (ppm)
m/z

Figure S8

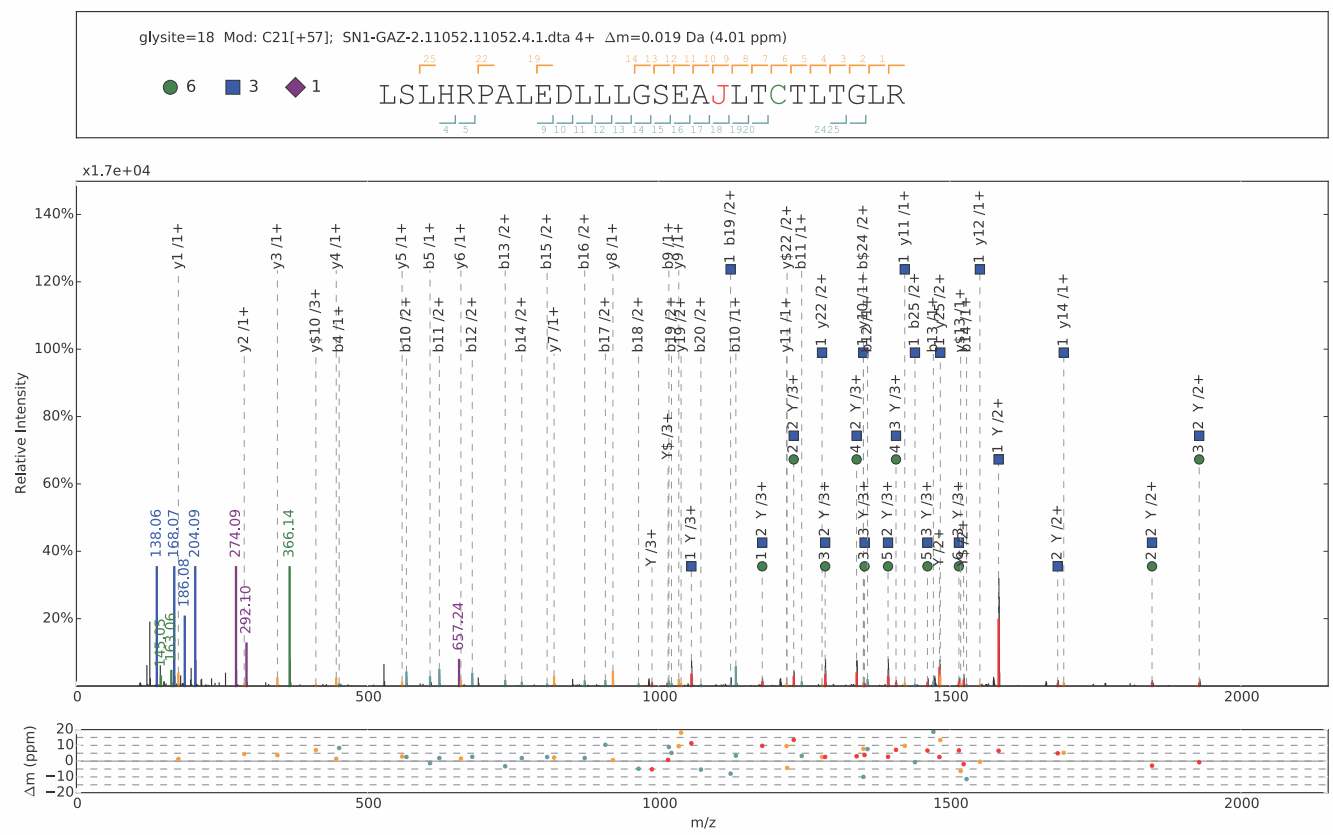
glysite=18 Mod: C21[+57]; SN1-GAZ-2.11052.11052.4.1.dta 4+ Δm=0.019 Da (4.01 ppm)
6
3
1
LSLHRPALEDLLLGSEAJLTCTLTGLR
x1.7e+04
Relative Intensity
140%
120%
100%
80%
60%
40%
20%
0
500
1000
1500
2000
Δm (ppm)
20
10
0
−10
−20
m/z